Supporting Information for: Aerosol oxidative potential and reactive species predicted with a chemical kinetics model (KM-OP)

Ashmi Mishra[1], Steven Lelieveld[1], Matteo Krüger[1], Steven J. Campbell[2], Deepchandra Srivastava[3], Grazia M. Lanzafame[4], Sophie Tomaz[5], Olivier Favez[4], Nicolas Bonnaire[6], Franco Lucarelli[7], Laurent Y. Alleman[8], Gaëlle Uzu[9], Jean-Luc Jaffrezo[9], Gang I. Chen[2], David C. Green[2], Max Priestman[2], Anja H. Tremper[2], Alexandre Barth[10], Markus Kalberer[10], Benjamin A. Musa Bandowe[1], Gerhard Lammel[1], Ulrich Pöschl[1], Pourya Shahpoury[11], Alexandre Albinet[4], and Thomas Berkemeier[1]

[1]Multiphase Chemistry Department, Max Planck Institute for Chemistry, 55128 Mainz, Germany
[2]MRC Centre for Environment and Health, Environmental Research Group, Imperial College London, 86 Wood Lane, London W12 0BZ, UK
[3]School of Geography, Earth Environmental Sciences, University of Birmingham, Edgbaston, Birmingham B15 2TT, United Kingdom
[4]Institut National de l'Environnement Industriel et des Risques (Ineris), Verneuil en Halatte, France
[5]INRS, 1 rue du Morvan CS 60027, 54519, Vandoeuvre-lès-Nancy, France
[6]Laboratoire des Sciences du Climat et de l'Environnement, CNRS-CEA-UVSQ, Gif-sur-Yvette, 91191, France
[7]University of Florence, Dipartimento di Fisica Astronomia, 50019 Sesto Fiorentino, Italy
[8]IMT Nord Europe, Université de Lille, Centre for Energy and Environnement, 59000 Lille, France
[9]Univ. Grenoble Alpes, IRD, CNRS, INRAE, Grenoble INP, IGE, UMR 5001, 38000, Grenoble, France
[10]Department of Environmental Sciences, University of Basel, 4056 Basel, Switzerland
[11]Environmental and Life Sciences, Trent University, Peterborough, Canada

Correspondence: Thomas Berkemeier (t.berkemeier@mpic.de) and Ashmi Mishra (a.mishra@mpic.de)

1 Supplementary Figures

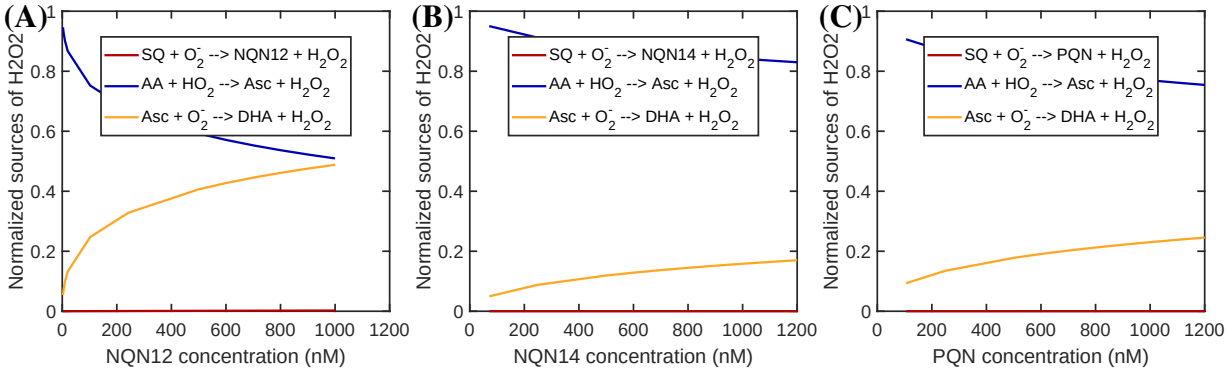

Figure S1. Normalized sources of H_2O_2 as a function of 1,2-NQN (A), 1,4-NQN (B) and PQN (C) concentrations.

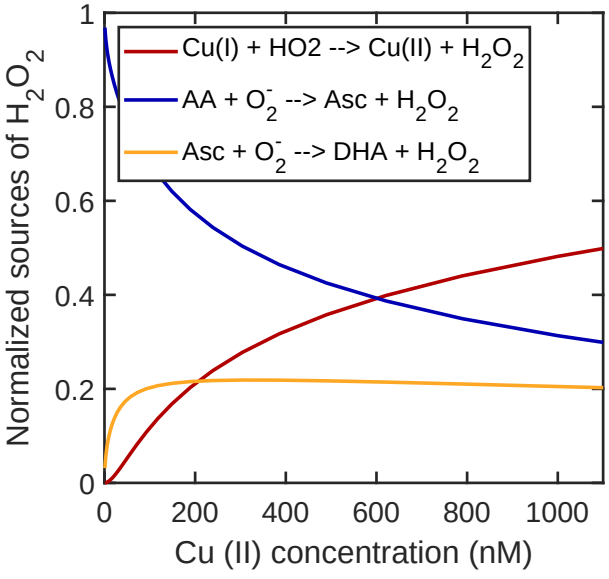

Figure S2. Normalized sources of H_2O_2 as a function of Cu concentration.

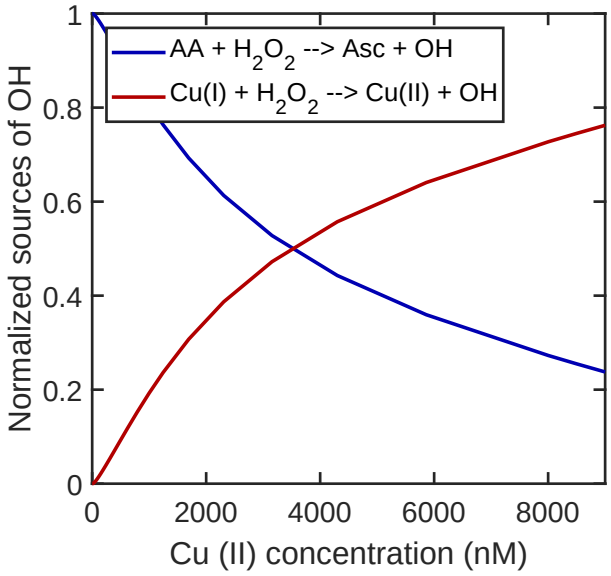

Figure S3. Normalized sources of OH as a function of Cu concentration.

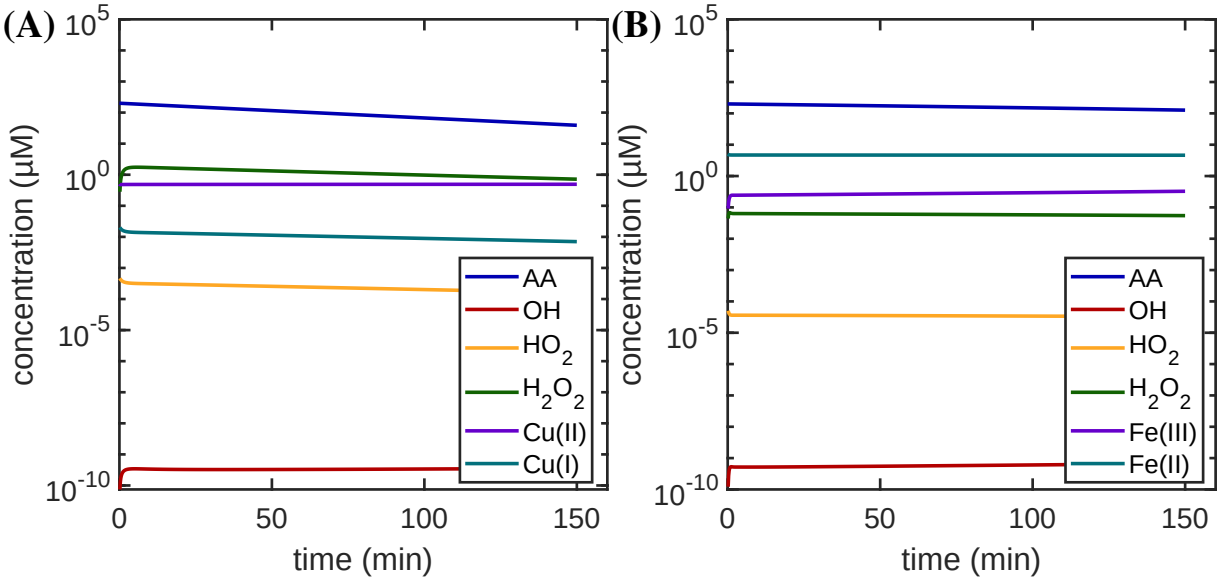

Figure S4. Concentration of ROS and TMs (Cu (A), Fe (B)) over time.

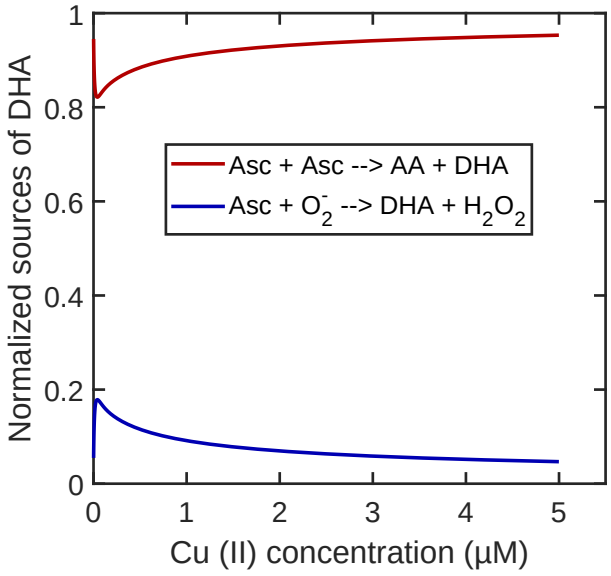

Figure S5. Normalized sources of DHA as a function of Cu concentration.

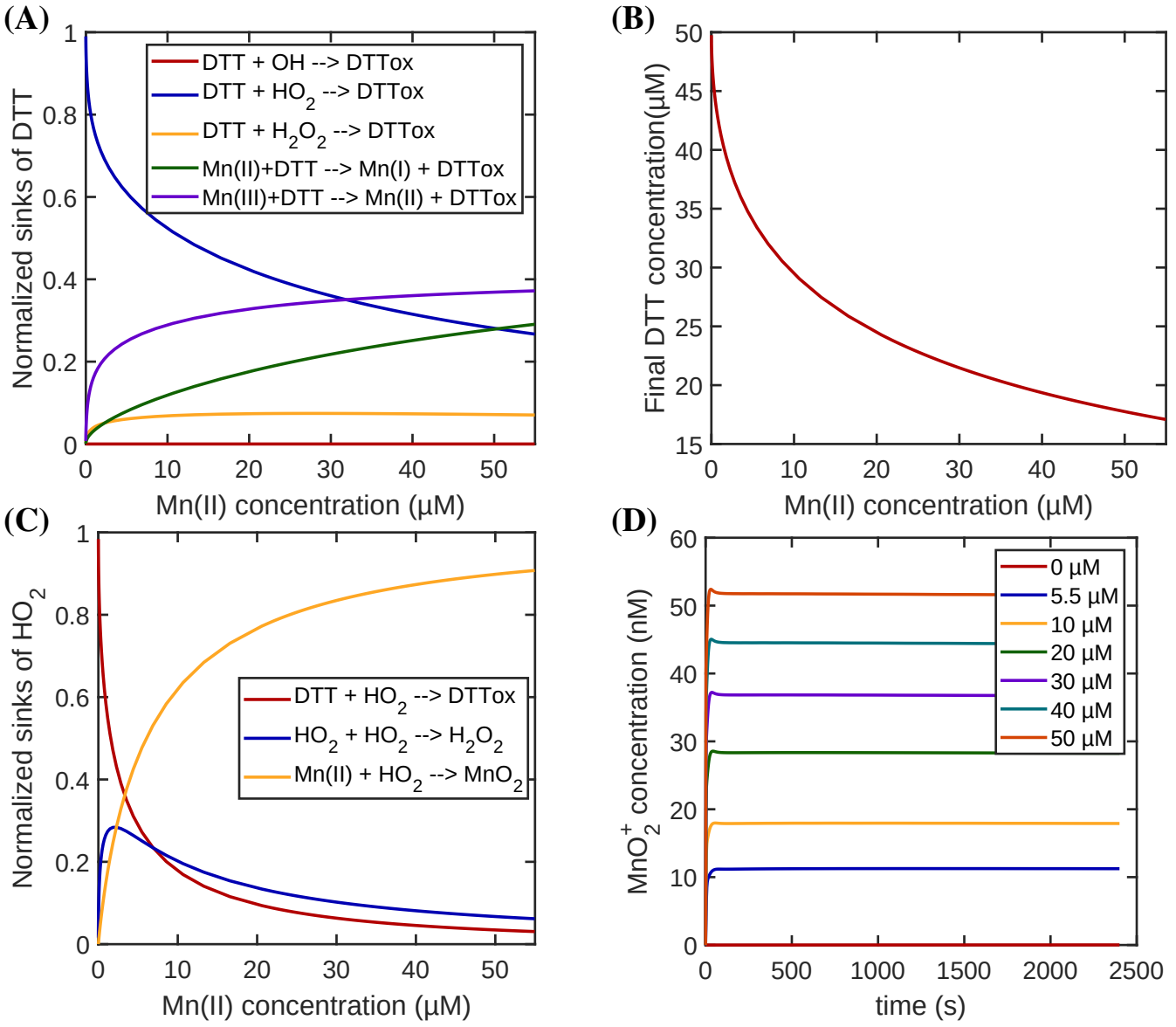

Figure S6. Normalized sinks of DTT (A), final DTT concentration (B), and normalized sinks of HO_2 (C) as a function of Mn concentration. Panel D shows the MnO_2^+ concentration over time.

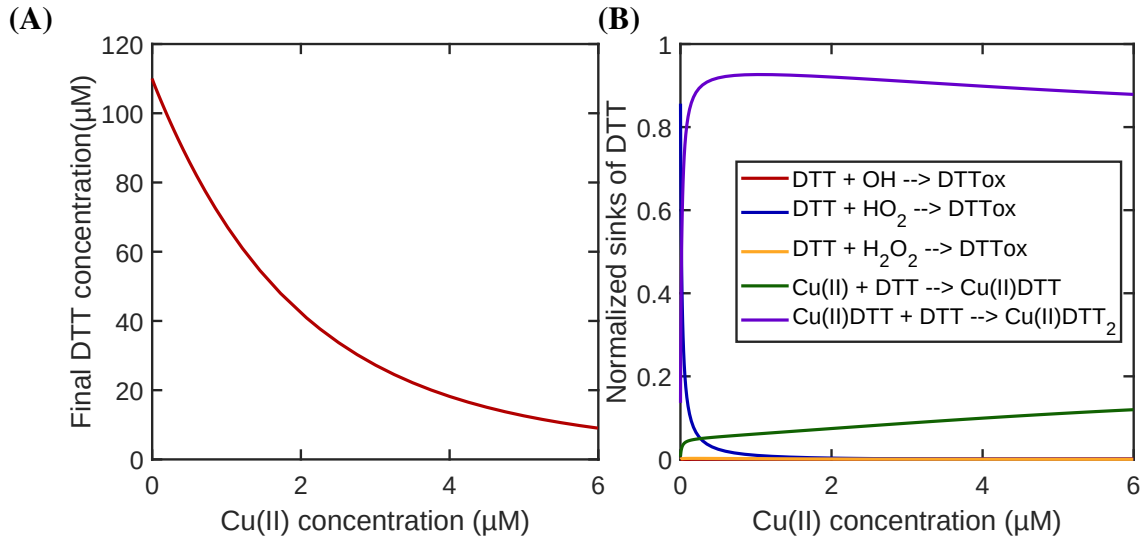

Figure S7. End concentration of DTT (A) and normalized sinks of DTT as a function of Cu concentration (B).

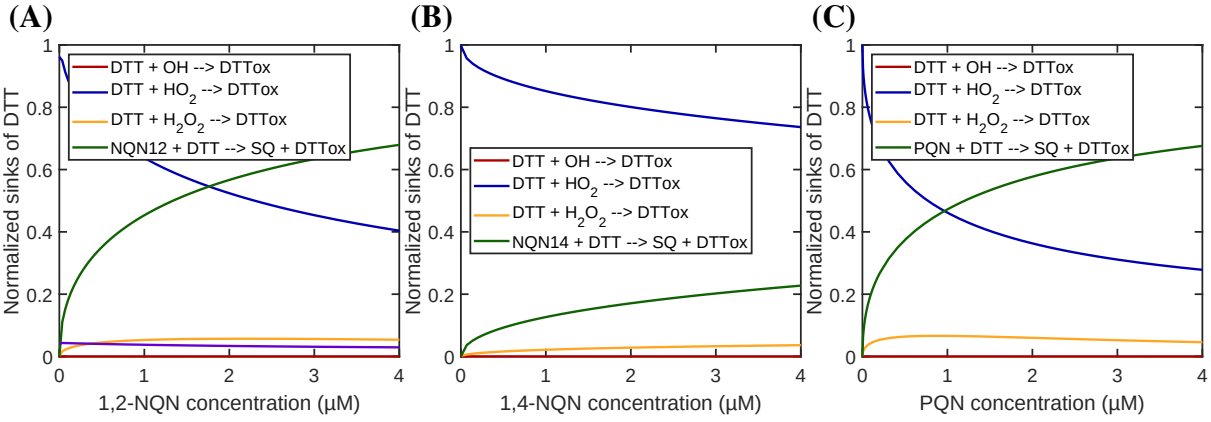

Figure S8. Normalized sinks of DTT as a function of 1,2-NQN (A), 1,4-NQN (B) and PQN (C) concentrations.

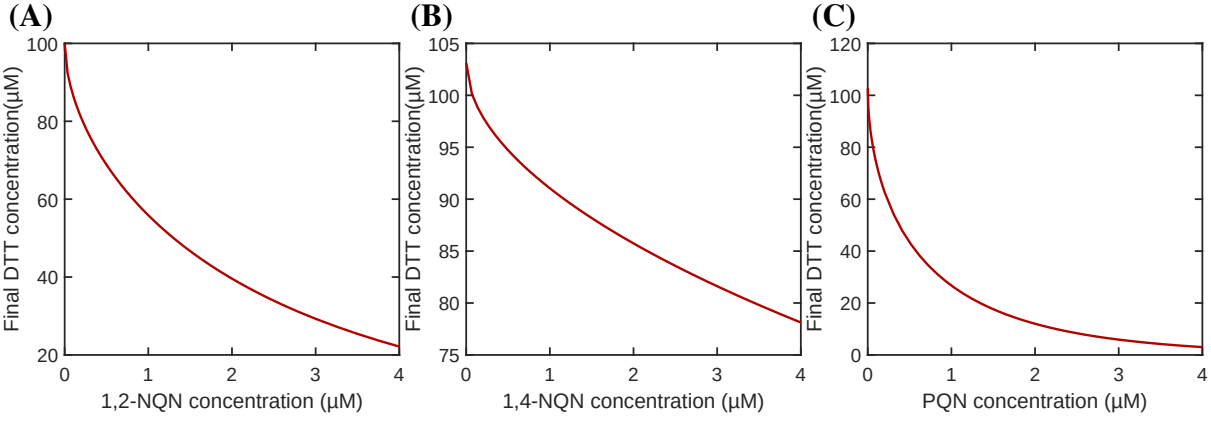

Figure S9. End concentration of DTT as a function of 1,2-NQN (A), 1,4-NQN (B) and PQN (C) concentrations.

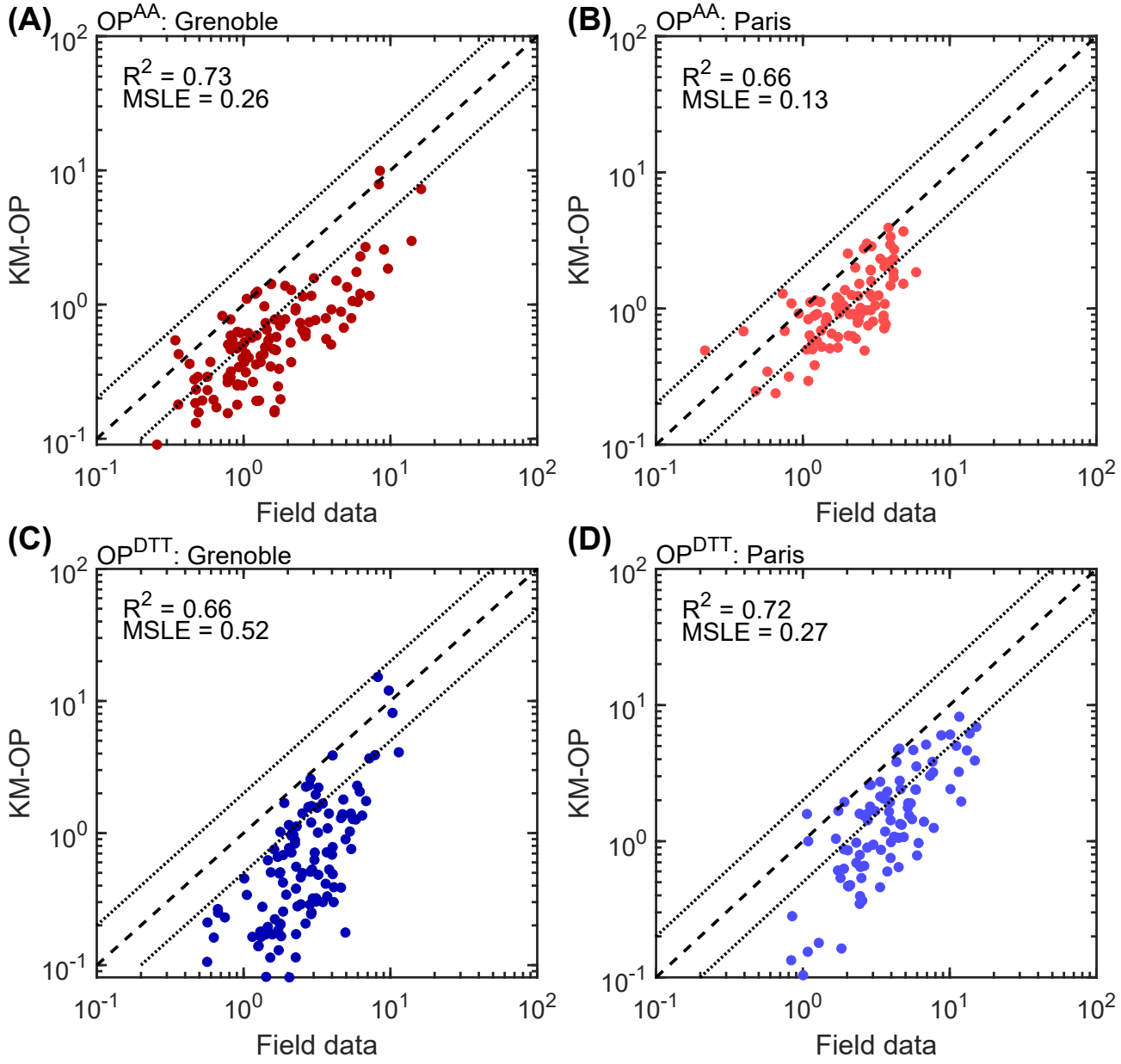

Figure S10. Correlation scatter plots of model-predicted and measured OP for particulate matter samples using source-apportioned SOA as input for samples from Grenoble (OP^{AA}: panel A, and OP^{DTT}: panel C) and Paris (OP^{AA}: panel B, and OP^{DTT}: panel D). Data shown in blue indicate OP^{DTT} (in units of nmol min^{-1} m^{-3}), while the red and pink data show OP^{AA} (in units of nmol min^{-1} m^{-3}) and OP^{DHA} (in units of nmol m^{-3}). The dashed lines indicate the 1:1 line. The dotted lines indicate the 2:1 and 1:2 lines. The error bars indicate the maximum and minimum values from the ensemble fits.

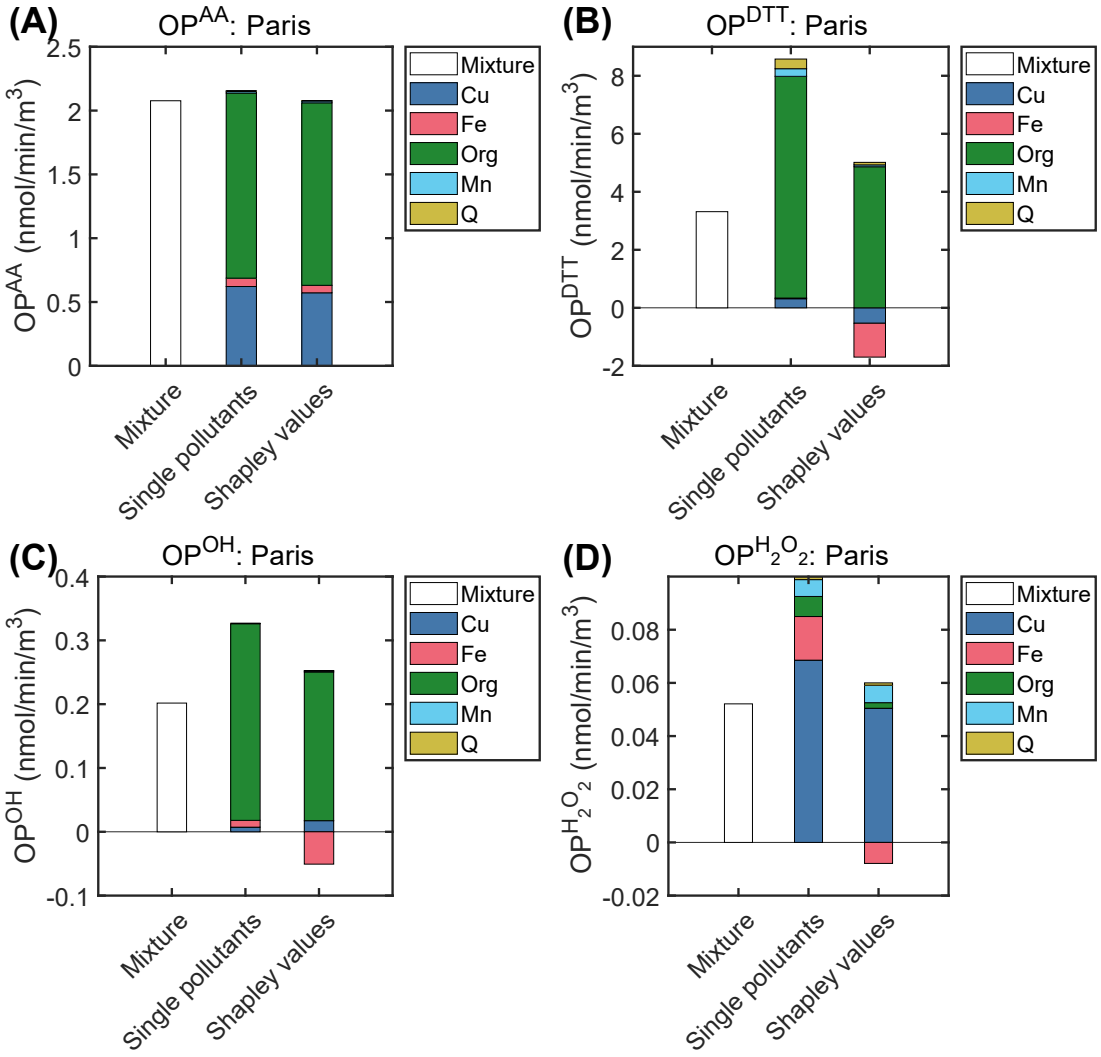

Figure S11. Contributions of different PM constituents to OP^{AA} (A), OP^{DTT} (B), OP^{OH} (C), and $OP^{H_2O_2}$ (D) in Paris. The "Mixture" bar shows the model result when all species are included in the model. The "Single pollutants" bar indicates a scenario where only one specific species was included. The "Shapley values" bar is calculated using the Shapley analysis.

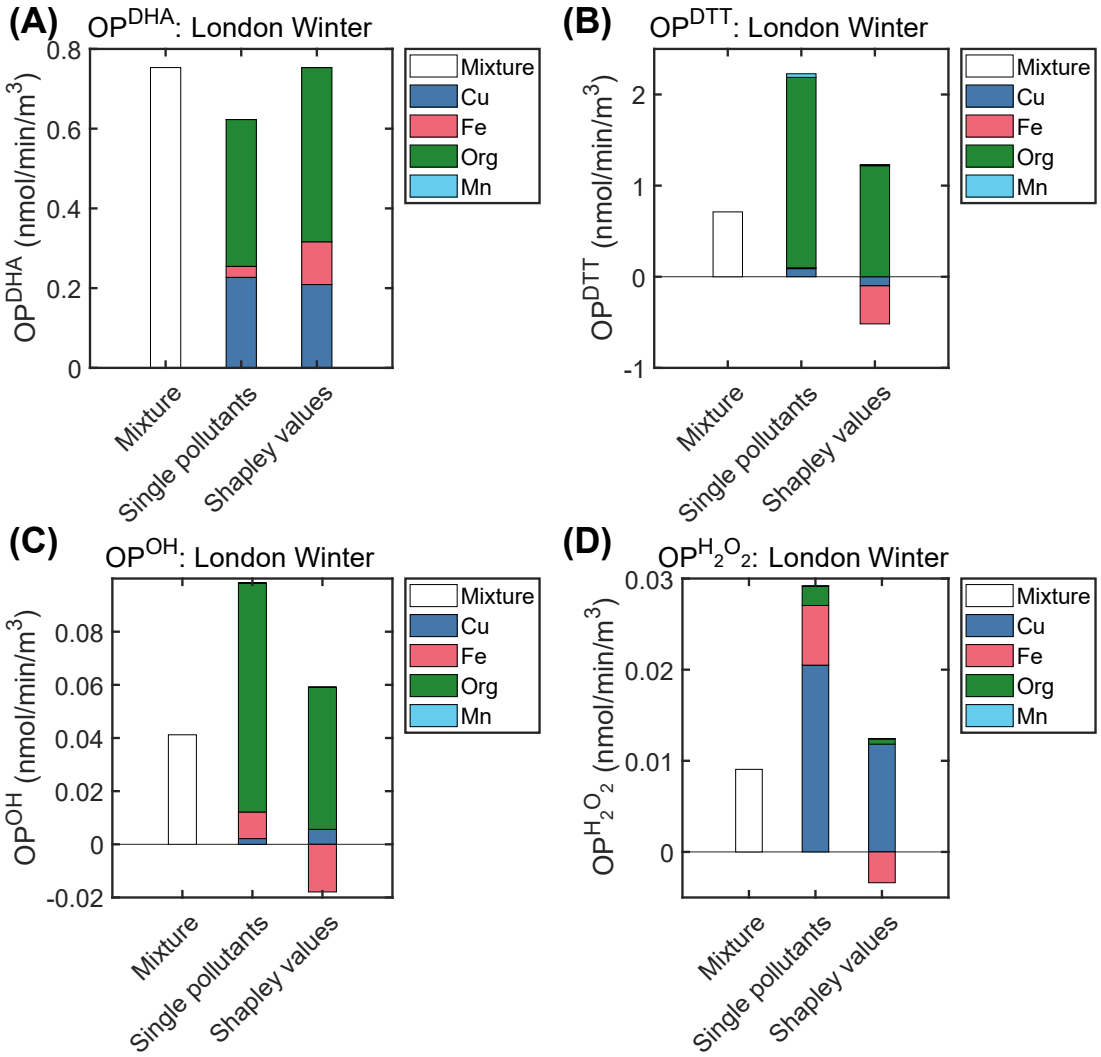

Figure S12. Contributions of different PM constituents to OP^{AA} (A), OP^{DTT} (B), OP^{OH} (C), and $OP^{H_2O_2}$ (D) in London during winter. The "Mixture" bar shows the model result when all species are inclmuded in the model. The "Single pollutants" bar indicates a scenario where only one specific species was included. The "Shapley values" bar is calculated using the Shapley analysis.

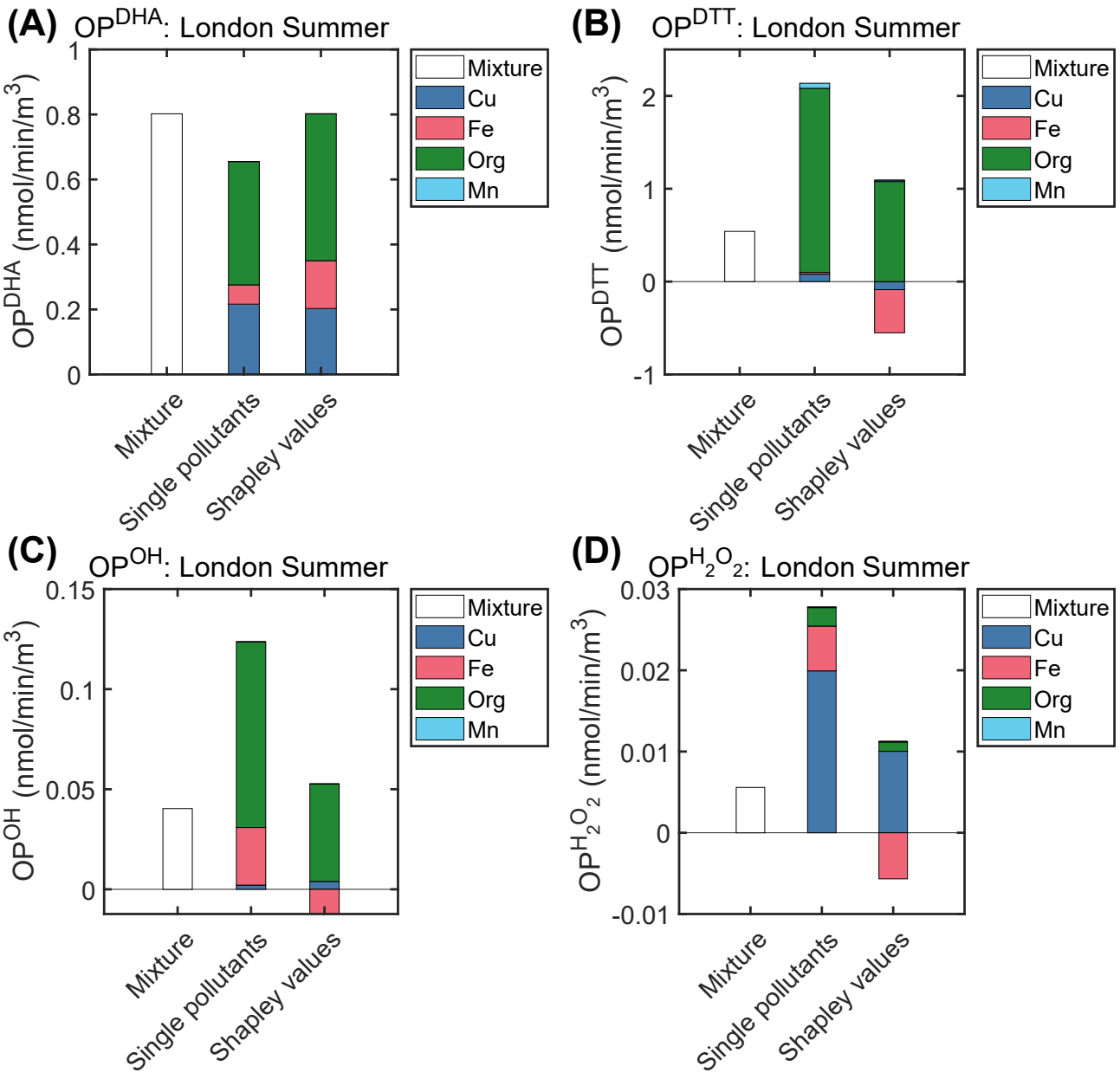

Figure S13. Contributions of different PM constituents to OP^{AA} (A), OP^{DTT} (B), OP^{OH} (C), and $OP^{H_2O_2}$ (D) in London during summer. The "Mixture" bar shows the model result when all species are included in the model. The "Single pollutants" bar indicates a scenario where only one specific species was included. The "Shapley values" bar is calculated using the Shapley analysis.

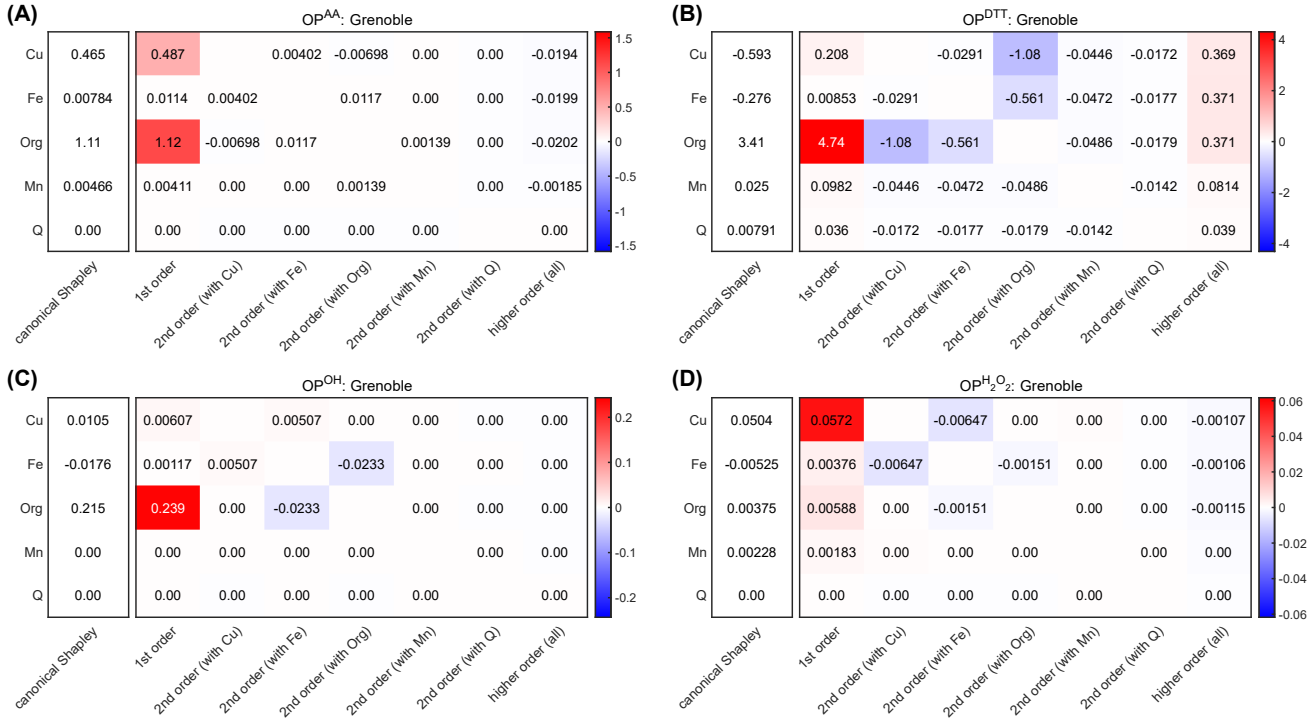

Figure S14. Deconvolution of the Shapley values into first and higher-order effects of PM constituents towards OP^{AA} (A), OP^{DTT} (B), OP^{OH} (C), and $OP^{H_2O_2}$ (D) in Grenoble.

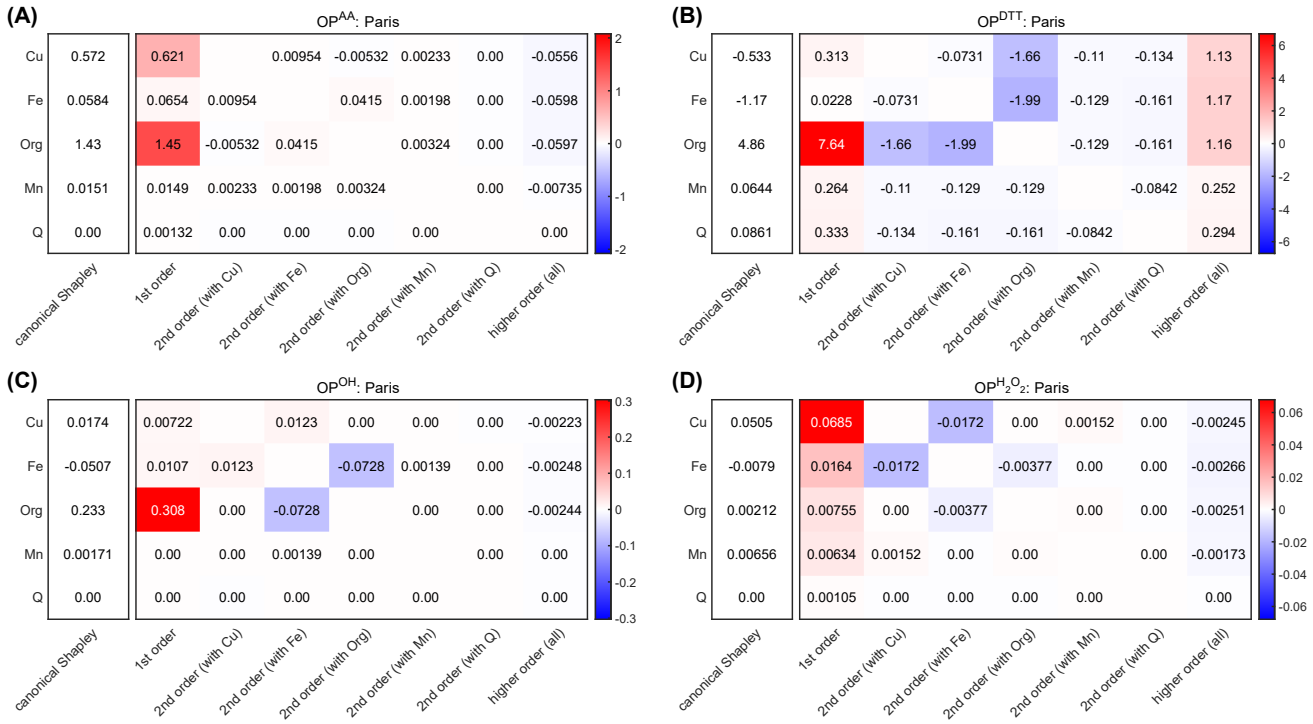

Figure S15. Deconvolution of the Shapley values into first and higher-order effects of PM constituents towards OP^{AA} (A), OP^{DTT} (B), OP^{OH} (C), and $OP^{H_2O_2}$ (D) in Paris.

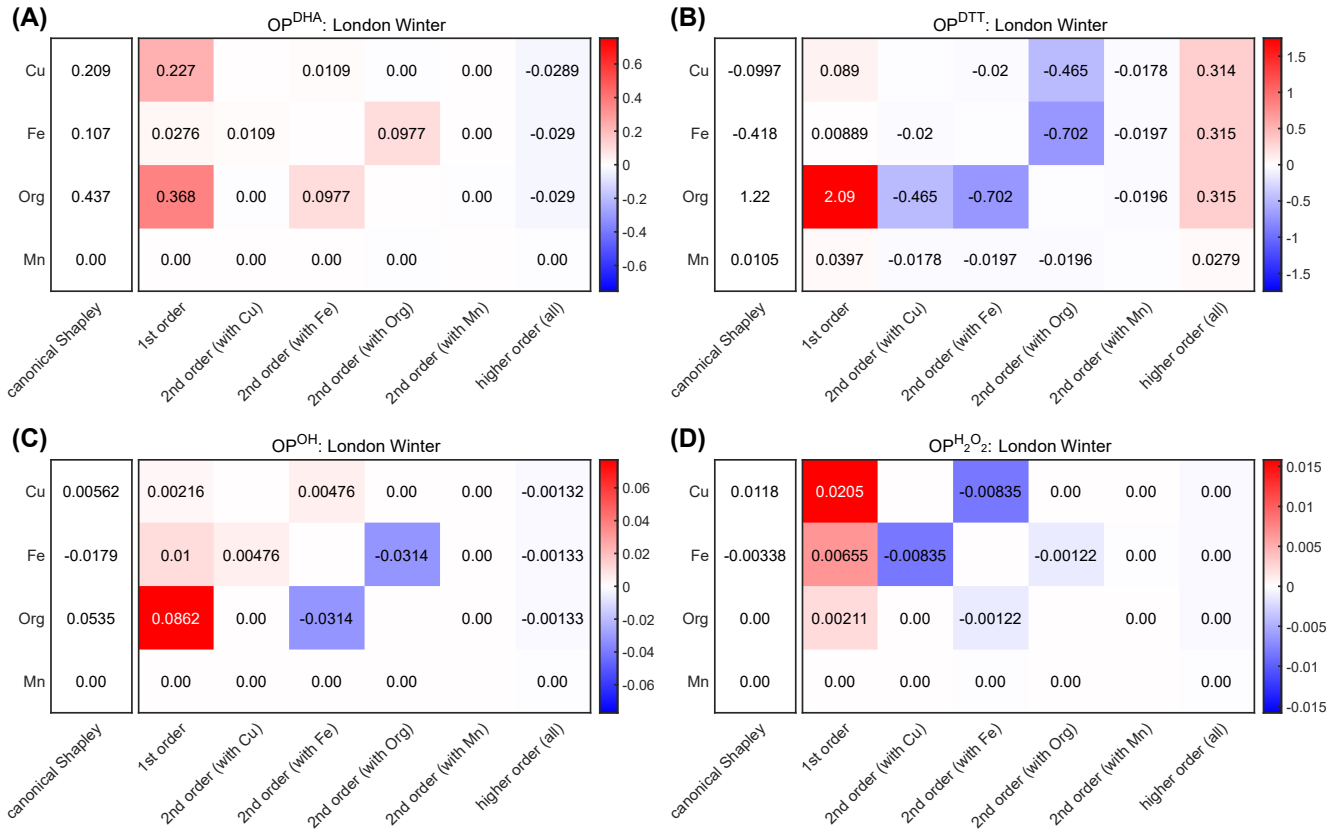

Figure S16. Deconvolution of the Shapley values into first and higher-order effects of PM constituents towards OP^{DHA} (A), OP^{DTT} (B), OP^{OH} (C), and $OP^{H_2O_2}$ (D) in London (during Winter).

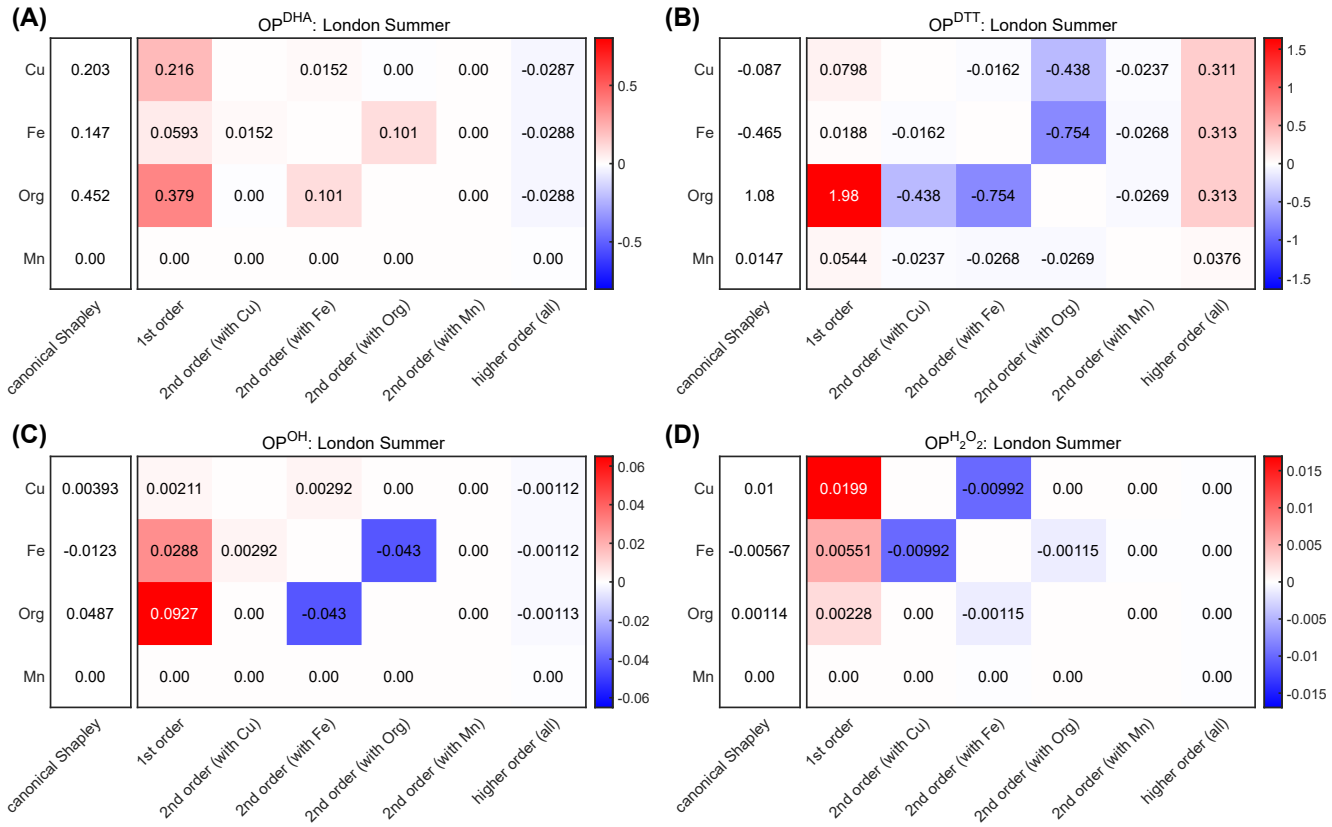

Figure S17. Deconvolution of the Shapley values into first and higher-order effects of PM constituents towards OP^{AA} (A), OP^{DTT} (B), OP^{OH} (C), and $OP^{H_2O_2}$ (D) in London (during Summer).

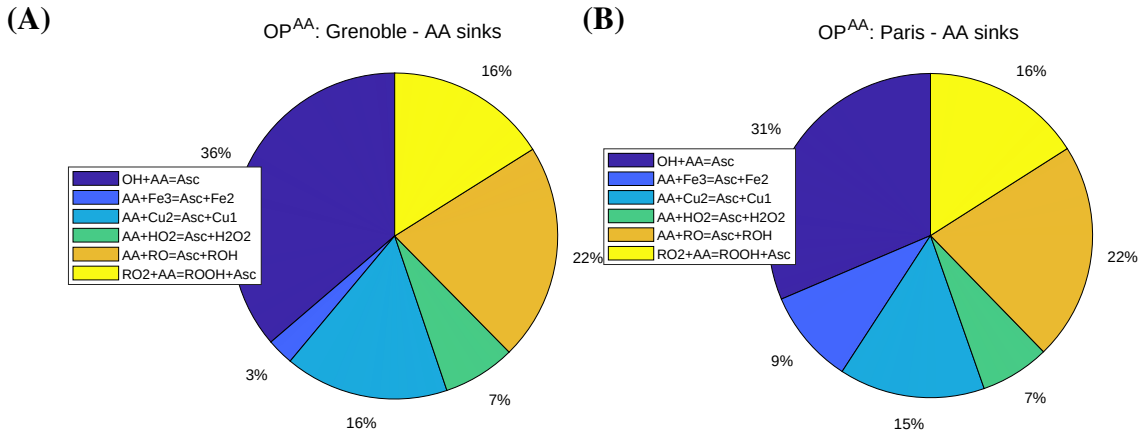

Figure S18. Main sinks of ascorbic acid for Grenoble (A) and Paris (B).

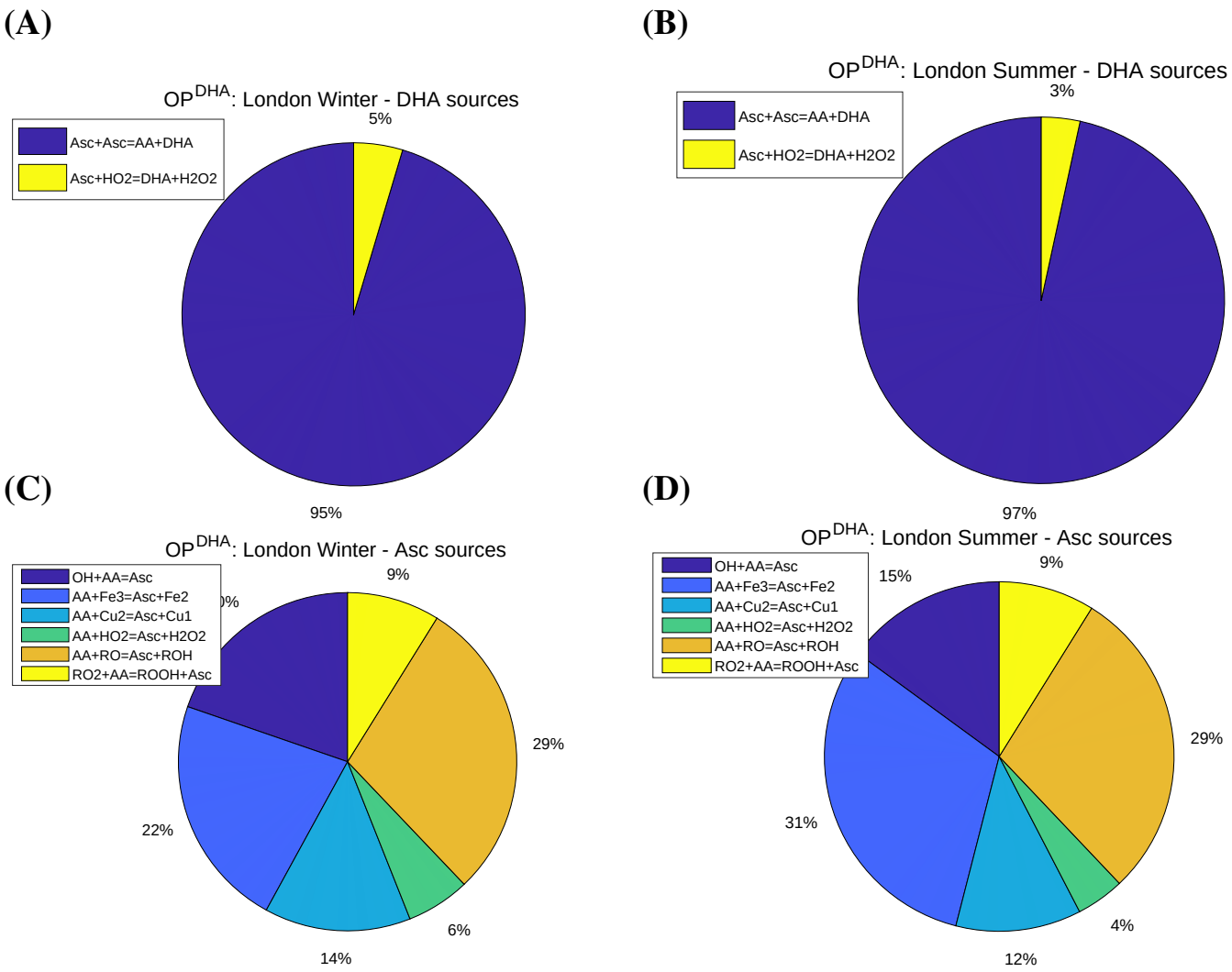

Figure S19. Main sources of dehydroascorbic acid for London winter (A) and London summer (B). Main sources of ascorbyl radical for London winter (C) and London summer (D).

(A) **(B)**

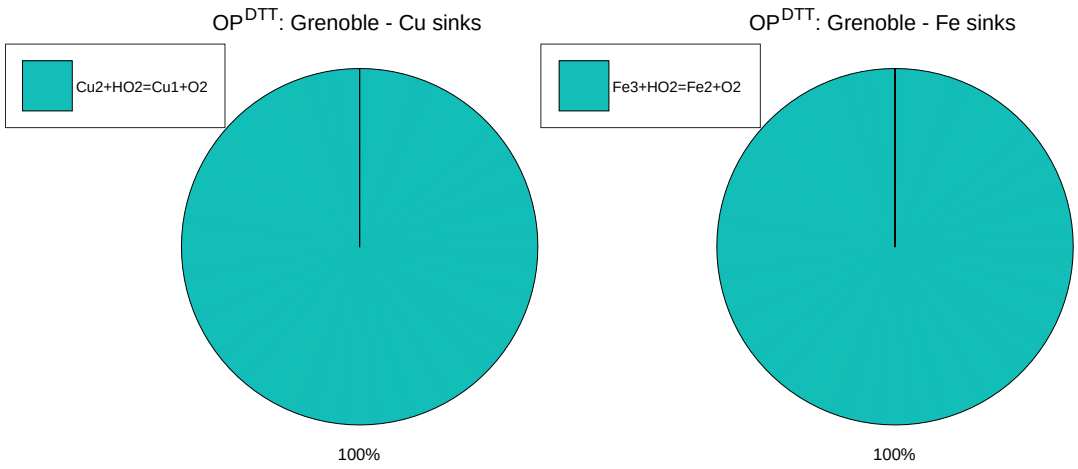

Figure S20. Main sinks of Cu(II) and Fe(III) in the DTT assay for Grenoble data.

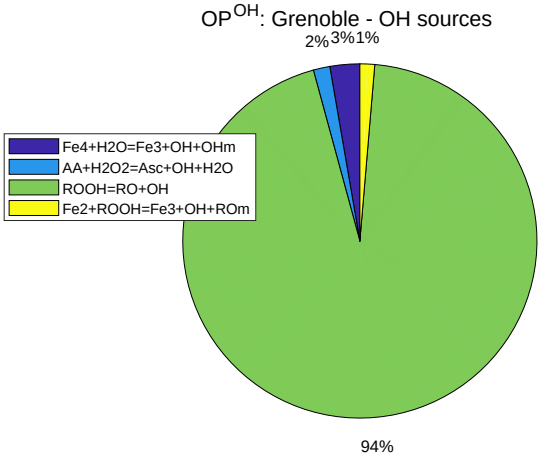

Figure S21. Main sources of OH for Grenoble data.

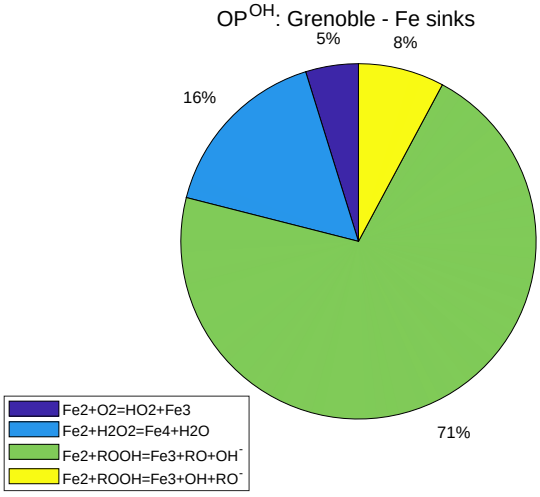

Figure S22. Main sinks of Fe(II) in the OH assay for Grenoble data.

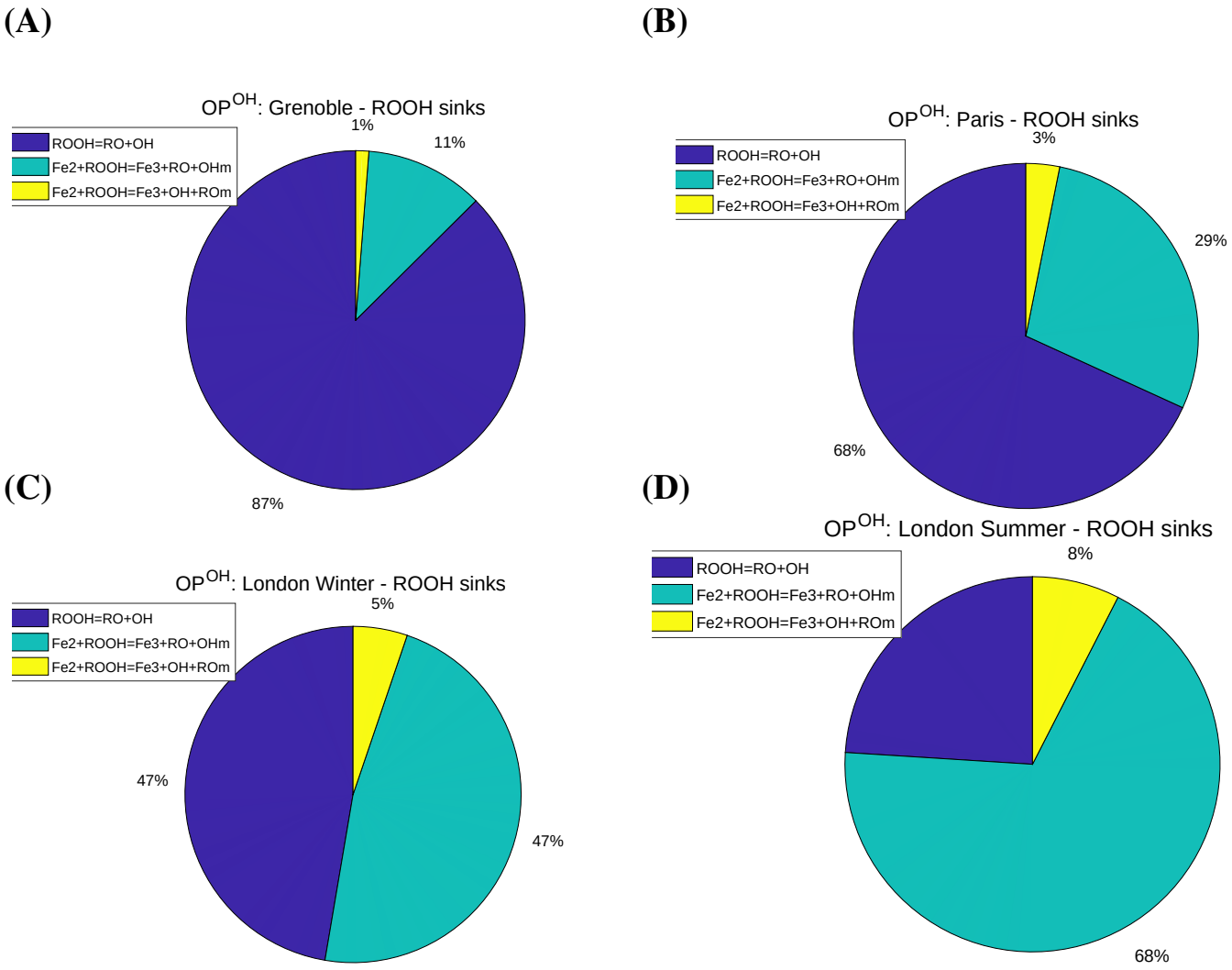

Figure S23. Main sinks of ROOH in the OH assay for Grenoble (A), Paris (B), London in winter (C) and London in summer (D).

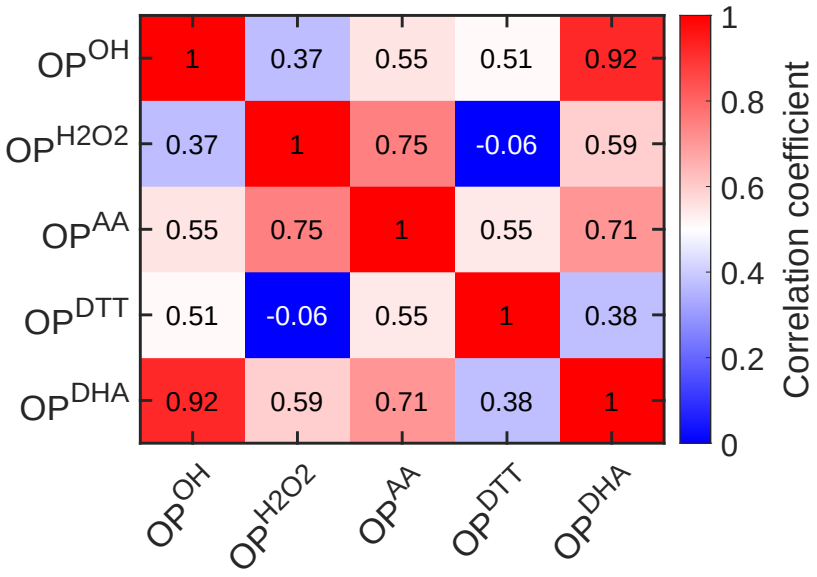

Figure S24. Correlation matrix between intrinsic OP assays in Grenoble.

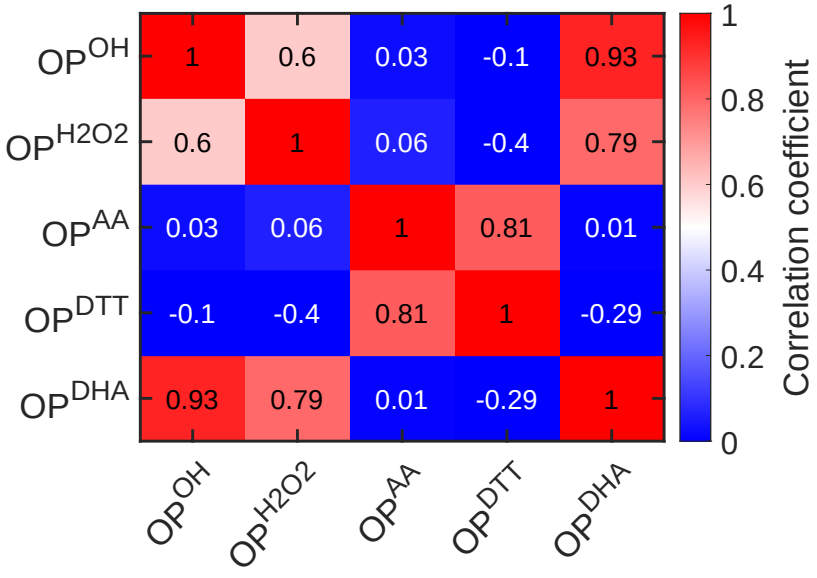

Figure S25. Correlation matrix between intrinsic OP assays in Paris.

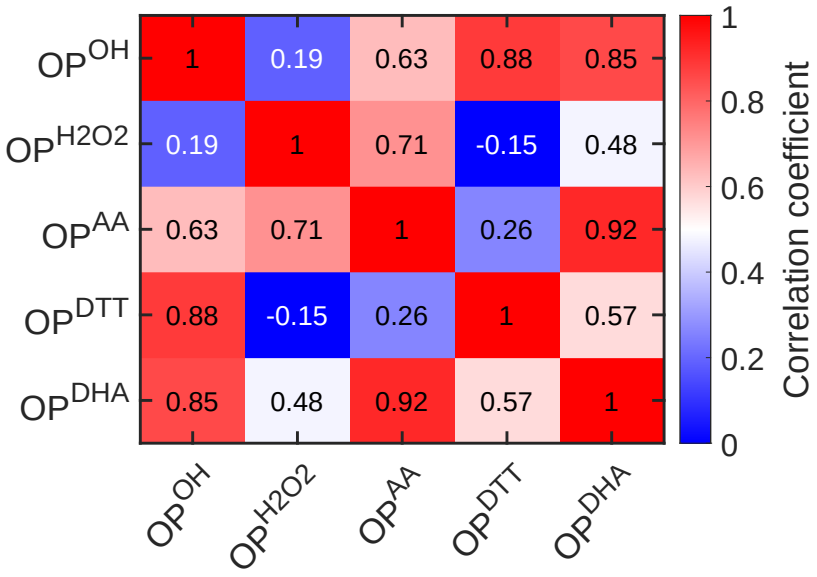

Figure S26. Correlation matrix between intrinsic OP assays in London during Winter.

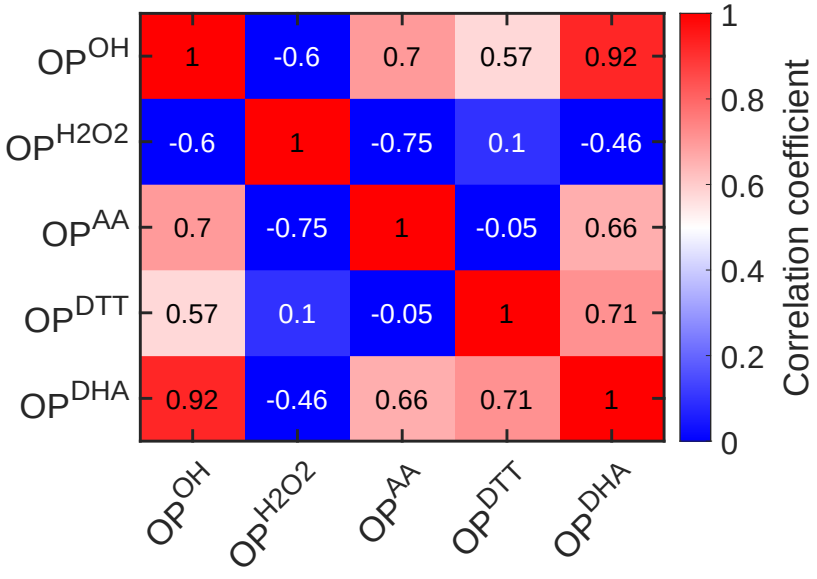

Figure S27. Correlation matrix between intrinsic OP assays in London during Summer.

2 Supplementary Tables

Table S1. Chemical reactions included in the KM-OP model. The respective lower and upper boundaries indicate the initial constraints of the fit ensemble. Values that were fixed during the fitting procedure are indicated using square brackets. Species in parenthesis in the chemical reaction refer to those that partake in the chemical reaction but that are not used to determine the reaction order. The rate coefficients are for 298 K in units of $cm^3\ s^{-1}$, unless otherwise noted. All reactions were assumed to have an activation energy (Ea) of 50 kJ mol^{-1}.

Reaction number	Reaction	Range	Reference
1	$OH + AA \rightarrow AA^{\bullet} + OH^-$	$[1.20 \times 10^{-11}]$	Shen et al. (2021)
2	$OH + UAH \rightarrow UA + OH^-$	$[1.20 \times 10^{-11}]$	Lakey et al. (2016)
3	$OH + GSH \rightarrow GS + OH^-$	$[1.70 \times 10^{-11}]$	Lakey et al. (2016)
4	$OH + GSSG \rightarrow GSSG^+ + OH^-$	$[1.20 \times 10^{-11}]$	Assumed to be fast
5	$OH + Cit \rightarrow NRP + \ + OH^-$	$[9.7 \times 10^{-14}]$	Liu et al. (2017)
6	$1,2-NQN + AA \rightarrow 1,2-NQN^{\bullet} + AA^{\bullet}$	$1.50 \times 10^{-22} - 1.50 \times 10^{-16}$	This study
7	$1,2-NQN^{\bullet} + O_2 \rightarrow 1,2-NQN + O_2^-$	$[1.35 \times 10^{-14}]$	This study
8	$1,2-NQN^{\bullet} + O_2^- (+ 2H^+) \rightarrow 1,2-NQN + H_2O_2$	$3.3 \times 10^{-15} - 3.3 \times 10^{-11}$	This study
9	$1,2-NQN^{\bullet} + Fe(III) \rightarrow 1,2-NQN + Fe(II)$	$1.00 \times 10^{-19} - 1.00 \times 10^{-13}$	This study
10	$1,4-NQN + AA \rightarrow 1,4-NQN^{\bullet} + AA^{\bullet}$	$1.50 \times 10^{-22} - 1.50 \times 10^{-16}$	This study
11	$1,4-NQN^{\bullet} + O_2 \rightarrow 1,4-NQN + O_2^-$	$[3.06 \times 10^{-14}]$	This study
12	$1,4-NQN^{\bullet} + O_2^- \ (+ 2H^+) \rightarrow 1,4-NQN + H_2O_2$	$3.3 \times 10^{-15} - 3.3 \times 10^{-11}$	This study
13	$PQN + AA \rightarrow PQN^{\bullet} + AA^{\bullet}$	$1.50 \times 10^{-22} - 1.50 \times 10^{-16}$	This study
14	$PQN^{\bullet} + O_2 \rightarrow PQN + O_2^-$	$[2.31 \times 10^{-14}]$	This study
15	$PQN^{\bullet} + O_2^- (+ 2H^+) \rightarrow PQN + H_2O_2$	$3.30 \times 10^{-15} - 3.30 \times 10^{-11}$	This study
16	$Fe(III) + AA \rightarrow Fe(II) + AA^{\bullet}$	$6.97 \times 10^{-21} - 6.97 \times 10^{-19}$	This study
17	$Fe(II) + O_2 \rightarrow Fe(III) + O_2^-$	$[4.48 \times 10^{-21}]$	Gonzalez et al. (2021)
18	$Fe(II) + O_2^- (+ 2H^+) \rightarrow Fe(III) + H_2O_2$	$[1.66 \times 10^{-14}]$	Ervens et al. (2003)
fe(II19	$Fe(II) + OH \rightarrow Fe(III) + OH^-$	$[5.81 \times 10^{-13}]$	Halliwell and Gutteridge (2015)
20	$Fe(III) + HO_2 \rightarrow Fe(II) + O_2 + H^+$	$[2.16 \times 10^{-16}]$	Ervens et al. (2003)
21	$Fe(III) + O_2^- \rightarrow Fe(II) + O_2$	$[2.49 \times 10^{-13}]$	Ervens et al. (2003)
22	$Fe(II) + H_2O_2 \rightarrow Fe(IV) + H_2O$	$8.14 \times 10^{-19} - 8.14 \times 10^{-17}$	This study
23	$Fe(II) + H_2O_2 \rightarrow Fe(III) + OH + OH^-$	$1.26 \times 10^{-20} - 1.26 \times 10^{-18}$	This study
24	$Fe(II) + Fe(IV) \rightarrow Fe(III) + Fe(III)$	$[6.60 \times 10^{-18}]$	Lakey et al. (2016)
25	$Fe(IV) \ (+ H_2O) \rightarrow Fe(III) + OH + OH^-$	$1.30 \times 10^{-4} - 1.30\ s^{-1}$	This study
26	$H_2O_2 + OH \rightarrow HO_2 + H_2O$	$[5.50 \times 10^{-14}]$	Lakey et al. (2016)
27	$OH + OH \rightarrow H_2O_2$	$[8.60 \times 10^{-12}]$	Lakey et al. (2016)
28	$OH + HO_2 \rightarrow O_2 + H_2O$	$[1.66 \times 10^{-11}]$	Ervens et al. (2003)
29	$HO_2 + HO_2 \rightarrow H_2O_2 + O_2$	$[1.40 \times 10^{-15}]$	Lakey et al. (2016)
30	$H_2O_2 + HO_2 \rightarrow H_2O_2 + O_2$	$[5.00 \times 10^{-21}]$	Lakey et al. (2016)
31	$HO_2 + O_2^- (+ H_2O) \rightarrow H_2O_2 + O_2 + OH^-$	$[1.70 \times 10^{-13}]$	Ervens et al. (2003)
32	$OH + O_2^- \rightarrow O_2 + OH^-$	$[1.83 \times 10^{-11}]$	Ervens et al. (2003)

Table S1. Continued.

Reaction number	Reaction	Range	Reference
33	$Cu(II) + AA \rightarrow Cu(I) + AA^{\bullet}$	1.46×10^{-19} – 1.46×10^{-17}	This study
34	$Cu(I) + O_2 \rightarrow Cu(II) + O_2^-$	[7.64×10^{-16}]	Ervens et al. (2003)
35	$Cu(I) + O_2^- (+ 2H^+) \rightarrow Cu(II) + H_2O_2$	1.56×10^{-12} – 1.56×10^{-10}	This study
36	$Cu(I) + OH \rightarrow Cu(II) + OH^-$	[4.98×10^{-12}]	Ervens et al. (2003)
37	$Cu(I) + H_2O_2 \rightarrow Cu(III) + OH^- + OH^-$	1.16×10^{-19} – 1.16×10^{-14}	This study
38	$Cu(I) + Cu(III) \rightarrow Cu(II) + Cu(II)$	[5.80×10^{-12}]	Lakey et al. (2016)
39	$Cu(II) + H_2O_2 \rightarrow Cu(I) + HO_2 + H^+$	7.64×10^{-19}	Pham et al. (2013)
40	$Cu(II) + O_2^- \rightarrow Cu(I) + O_2$	[1.83×10^{-11}]	Ervens et al. (2003)
41	$Cu(II) + HO_2 \rightarrow Cu(I) + O_2 + H^+$	[1.66×10^{-13}]	Ervens et al. (2003)
42	$Cu(I) + HO_2 \rightarrow Cu(II) + O_2 + H^+$	[4.98×10^{-12}]	Ervens et al. (2003)
43	$Cu(III)\ (+ H_2O) \rightarrow Cu(II) + OH + OH^-$	2.32×10^{-3} – $2.32\ s^{-1}$	This study
44	$AA^{\bullet} + AA^{\bullet} \rightarrow AA + DHA$	[5.00×10^{-16}]	Lakey et al. (2016)
45	$AA + GS \rightarrow AA^{\bullet} + GSH$	[1.00×10^{-12}]	Lelieveld et al. (2021)
46	$AA + UA \rightarrow AA^{\bullet} + UAH$	[1.70×10^{-15}]	Lelieveld et al. (2021)
47	$UAH + GS \rightarrow UA + GSH$	[5.00×10^{-14}]	Lelieveld et al. (2021)
48	$AA + H_2O_2 \rightarrow AA^{\bullet} + OH + OH^-$	2.19×10^{-23} – 2.19×10^{-19}	This study
49	$AA + HO_2\ (+ H^+) \rightarrow AA^{\bullet} + H_2O_2$	[2.65×10^{-17}]	Lelieveld et al. (2021)
50	$AA + O_2^-\ (+ 2H^+) \rightarrow AA^{\bullet} + H_2O_2$	[5.10×10^{-17}]	Lelieveld et al. (2021)
51	$OH + Benzoate \rightarrow BenzOH$	[1.00×10^{-11}]	Lakey et al. (2016)
52	$O_2^- + O_2^-\ (+ 2H^+) \rightarrow H_2O_2 + O_2$	[2.49×10^{-14}]	Kohen and Nyska (2002)
53	$GSH + H_2O_2 \rightarrow GSSG + O_2$	[1.44×10^{-21}]	Lelieveld et al. (2021)
54	$GS^- + H_2O_2 \rightarrow GSOH + O_2$	[1.60×10^{-21}]	Lelieveld et al. (2021)
55	$HO_2 + GSH \rightarrow GS + H_2O_2$	[3.32×10^{-19}]	Lelieveld et al. (2021)
56	$Cu(I) + H_2O_2 \rightarrow Cu(II) + OH + OH^-$	1.16×10^{-19} – 1.16×10^{-15}	This study
57	$DTT + OH \rightarrow DTT^{\bullet} + H_2O$	[1.66×10^{-11}]	Netto and Stadtman (1996)
58	$DTT + HO_2 \rightarrow DTT^{\bullet} + 2\,OH^-$	2.65×10^{-17} – 2.65×10^{-13}	This study
59	$DTT + H_2O_2 \rightarrow DTT^{\bullet} + H_2O + OH^-$	[3.04×10^{-21}]	Netto and Stadtman (1996)
60	$Fe(III) + DTT \rightarrow DTT^{\bullet} + Fe(II)$	4.65×10^{-21}	Netto and Stadtman (1996)
61	$Cu(II) + DTT \rightarrow [Cu^{2+}(DTT^{2-})]$	2.00×10^{-21} – 2.00×10^{-17}	This study
62	$[Cu^{2+}(DTT^{2-})] + DTT \rightarrow [Cu^{2+}(DTT^{2-})_2]^{2-}$	2.00×10^{-19} – 2.00×10^{-15}	This study

Table S1. Continued.

Reaction number	Reaction	Range	Reference
63	$[Cu^{2+}(DTT^{2-})_2]^{2-} \rightarrow [Cu^{+}(DTT^{2-})(DTT^{\bullet-})]^{2-}$	$2.00 \times 10^{-3} - 2.00 \times 10^{1}$ s^{-1}	This study
64	$[Cu^{+}(DTT^{2-})(DTT^{\bullet-})]^{2-} + O_2 \rightarrow [Cu^{+}(DTT^{2-})(DTTOO^{\bullet-})]^{2-}$	$2.00 \times 10^{-19} - 2.00 \times 10^{-15}$	This study
65	$[Cu^{+}(DTT^{2-})(DTTOO^{\bullet-})]^{2-} + DTT \rightarrow [Cu^{2+}(DTT^{2-})] + 2\,RSSR$	$2.00 \times 10^{-18} - 2.00 \times 10^{-14}$	This study
66	$[Cu^{2+}(DTT^{2-})] \rightarrow [Cu^{+}(DTT^{\bullet-})]$	$2.00 \times 10^{-3} - 2.00 \times 10^{1}$ s^{-1}	This study
67	$[Cu^{+}(DTT^{\bullet-})] + O_2 \rightarrow [Cu^{+}(DTTOO^{\bullet-})]$	$2.00 \times 10^{-23} - 2.00 \times 10^{-19}$	This study
68	$[Cu^{+}(DTTOO^{\bullet}-)] \rightarrow Cu(I) + RSSR$	$2.00 \times 10^{-6} - 2.00 \times 10^{-2}$ s^{-1}	This study
69	$Fe(IV) + DTT \rightarrow Fe(III) + DTT^{\bullet}$	$5.00 \times 10^{-19} - 5.00 \times 10^{-15}$	This study
70	$DTT^{\bullet} + DTT \rightarrow RSSR^{\bullet-}$	$1.00 \times 10^{-14} - 1.00 \times 10^{-11}$	This study
71	$DTT^{\bullet} + O_2 \rightarrow RSS + HO_2$	$[1.18 \times 10^{-12}]$	This study
72	$1,2-NQN + DTT \rightarrow 1,2-NQN^{\bullet} + DTT^{\bullet}$	$8.00 \times 10^{-23} - 8.00 \times 10^{-17}$	This study
73	$RSSR^{\bullet-} + 1,2-NQN \rightarrow RSSR + 1,2-NQN^{\bullet}$	$1.00 \times 10^{-19} - 1.00 \times 10^{-13}$	This study
74	$DTT^{\bullet} + 1,2-NQN \rightarrow RS-1,2-NQN$	$1.00 \times 10^{-18} - 1.00 \times 10^{-12}$	This study
75	$1,4-NQN + DTT \rightarrow 1,4-NQN^{\bullet} + DTT^{\bullet}$	$5.00 \times 10^{-24} - 5.00 \times 10^{-18}$	This study
76	$RSSR^{\bullet-} + 1,4-NQN \rightarrow RSSR + 1,4-NQN^{\bullet}$	$1.00 \times 10^{-19} - 1.00 \times 10^{-13}$	This study
77	$DTT^{\bullet} + 1,4-NQN \rightarrow RS-1,4-NQN$	$1.00 \times 10^{-18} - 1.00 \times 10^{-12}$	This study
78	$PQN + DTT \rightarrow PQN^{\bullet} + DTT^{\bullet}$	$6.00 \times 10^{-22} - 6.00 \times 10^{-16}$	This study
79	$RSSR^{\bullet-} + PQN \rightarrow RSSR + PQN^{\bullet}$	$1.00 \times 10^{-19} - 1.00 \times 10^{-13}$	This study
80	$DTT^{\bullet} + PQN \rightarrow RS-PQN$	$10^{-18} - 1.00 \times 10^{-12}$	This study
81	$AA^{\bullet} + O_2{}^{-} (+ 2H^{+}) \rightarrow DHA + H_2O_2$	$1.00 \times 10^{-16} - 1.00 \times 10^{-12}$	This study
82	$DHA + OH (+ 2H^{+}) \rightarrow NRP$	$[1.66 \times 10^{-11}]$	Shen et al. (2021)
83	$DHA + H_2O_2 \rightarrow NRP$	$[6.97 \times 10^{-23}]$	Shen et al. (2021)
84	$DHA (+ H_2O) \rightarrow DKG$	$4.8 \times 10^{-6} - 4.8 \times 10^{-2}$ s^{-1}	This study
85	$Mn(II) + DTT \rightarrow Mn(I) + DTT^{\bullet}$	$5.00 \times 10^{-23} - 5.00 \times 10^{-19}$	This study
86	$RSSR^{\bullet-} + O_2 \rightarrow RSSR + HO_2$	$[1.00 \times 10^{-12}]$	Kumagai et al. (2002)
87	$Mn(II) + OH \rightarrow Mn(III) + OH^{-}$	$[3.32 \times 10^{-14}]$	Jacobsen et al. (1998)
88	$Mn(II) + HO_2 \rightarrow MnO_2{}^{+} + H^{+}$	$1.00 \times 10^{-17} - 1.00 \times 10^{-13}$	Jacobsen et al. (1998)
89	$MnO_2{}^{+} + MnO_2{}^{+} (+ 2H^{+}) \rightarrow 2\,Mn(II) + H_2O_2 + O_2$	$[9.96 \times 10^{-15}]$	Morgan (2005)
90	$Mn(III) + H_2O_2 \rightarrow Mn(II) + HO_2 + H^{+}$	$[1.21 \times 10^{-16}]$	Jacobsen et al. (1998)
91	$Mn(III) + H_2O_2 \rightarrow MnO_2{}^{+} + 2\,H^{+}$	$[4.65 \times 10^{-18}]$	Jacobsen et al. (1998)
92	$MnO_2{}^{+} + HO_2 (+ H^{+}) \rightarrow Mn(II) + H_2O_2$	$[1.66 \times 10^{-14}]$	Halliwell and Gutteridge (2015)

Table S1. Continued.

Reaction number	Reaction	Range	Reference
93	$Mn(III) + DTT \rightarrow Mn(II) + DTT^{\bullet}$	$5.00 \times 10^{-17} - 5.00 \times 10^{-15}$	This study
94	$Mn(II) + O_2\ (+ H^+) \rightarrow Mn(III) + HO_2$	$[3.98 \times 10^{-21}]$	Halliwell and Gutteridge (2015)
95	$PQN + DTT \rightarrow RSSR + PQN^{\bullet}$	$1.00 \times 10^{-21} - 1.00 \times 10^{-17}$	This study
96	$RS-1,4-NQN + DTT \rightarrow RSSR + 1,4-NQN^{\bullet}$	$1.00 \times 10^{-21} - 1.00 \times 10^{-17}$	This study
97	$RS-1,2-NQN + DTT \rightarrow RSSR + 1,2-NQN^{\bullet}$	$1.00 \times 10^{-21} - 1.00 \times 10^{-17}$	This study
98	$GSOO + GSOO \rightarrow 0.56\,HO_2$	$[6.79 \times 10^{-13}]$	Lelieveld et al. (2021)
99	$GSOO + GSH \rightarrow GSO + GSOH$	$[3.32 \times 10^{-15}]$	Lelieveld et al. (2021)
100	$GS + GSH \rightarrow GSSG^-$	$[1.59 \times 10^{-14}]$	Lelieveld et al. (2021)
101	$GSSG^- \rightarrow GS$	$[1.60 \times 10^{5}\ s^{-}1]$	Lelieveld et al. (2021)
102	$GSSG^- + O_2\ (+ H_2O) \rightarrow GSSG + O_2^-$	$[8.30 \times 10^{-12}]$	Lelieveld et al. (2021)
103	$GS + GS \rightarrow GSSG$	$[8.30 \times 10^{-12}]$	Lelieveld et al. (2021)
104	$GSOH + GSH \rightarrow GSSG + H_2O$	$[1.20 \times 10^{-18}]$	Lelieveld et al. (2021)
105	$GSO + GSO \rightarrow NRP$	$[9.96 \times 10^{-14}]$	Lelieveld et al. (2021)
106	$GSH + Cu(II) \rightarrow [Cu^{2+}(GSH)]$	$1.00 \times 10^{-20} - 1.00 \times 10^{-16}$	This study
107	$Cu^{2+}(GSH) + GSH \rightarrow [Cu^{2+}(GSH)(GSH)]$	$1.00 \times 10^{-19} - 1.00 \times 10^{-15}$	This study
108	$2[Cu^{2+}(GSH)_2] + O_2 \rightarrow 2[Cu^{2+}(GS)(GSH)] + H_2O_2$	$2.00 \times 10^{-36} - 2.00 \times 10^{-32}\ cm^6\ s^{-1}$	This study
109	$2[Cu^{2+}(GS)(GSH)] + O_2 \rightarrow 2[Cu^{2+}(GS)(GS)] + H_2O_2$	$2.00 \times 10^{-41} - 2.00 \times 10^{-37}\ cm^6\ s^{-1}$	This study
110	$[Cu^{2+}(GS)(GS)] \rightarrow Cu(II) + GSSG$	$2.00 \times 10^{-4}\ s^{-1}$	This study
111	$ROOH \rightarrow RO + OH$	$[1.50 \times 10^{-3}\ s^{-1}]$	Campbell et al. (2023)
112	$OH + ROOH \rightarrow ROH + HO_2$	$[1.00 \times 10^{-16}]$	Campbell et al. (2023)
113	$RO \rightarrow R$	$[5.00 \times 10^{5}\ s^{-1}]$	Campbell et al. (2023)
114	$R + O_2 \rightarrow RO_2$	$[7.97 \times 10^{-12}]$	Campbell et al. (2023)
115	$AA + RO \rightarrow AA^{\bullet} + ROH$	$[2.01 \times 10^{-17}]$	Campbell et al. (2023)
116	$Fe(II) + ROOH \rightarrow Fe(III) + RO + OH^-$	$[6.64 \times 10^{-17}]$	Campbell et al. (2023)
117	$Fe(II) + ROOH \rightarrow Fe(III) + OH + RO^-$	$[7.31 \times 10^{-18}]$	Campbell et al. (2023)
118	$DTT + RO \rightarrow DTT^{\bullet} + ROH$	$[1.66 \times 10^{-17}]$	Assumed to be the same as 116
119	$Org + OH \rightarrow H_2O + R$	$[1.66 \times 10^{-13}]$	Campbell et al. (2023)
120	$Org + RO \rightarrow ROH + R$	$[1.33 \times 10^{-16}]$	Walling (1967)
121	$ROOH + RO \rightarrow ROH + RO_2$	$[5.48 \times 10^{-16}]$	Assumed to be the same as 112
122	$R + R \rightarrow product$	$[2.00 \times 10^{-14}]$	Wei et al. (2022)

Table S1. Continued.

Reaction number	Reaction	Range	Reference
123	$RO + RO \rightarrow ROOR$	[2.32×10^{-12}]	Walling (1967)
124	$RO_2 + RO_2 \rightarrow RO + RO + O_2$	[2.16×10^{-13}]	Mouchel-Vallon et al. (2017)
125	$RO_2 + RO_2 \rightarrow$ carbonyl + carbonyl + H_2O_2	[4.98×10^{-14}]	Mouchel-Vallon et al. (2017)
126	Fe(II) + $ROOR \rightarrow$ Fe(III) + RO + RO^-	[5.00×10^{-23}]	Wei et al. (2022)
127	$R + O_2 \rightarrow RO_2$	[7.64×10^{-12}]	Chevallier et al. (2004)
128	$RO_2 + HO_2 \rightarrow ROOH + O_2$	[6.97×10^{-16}]	Mouchel-Vallon et al. (2017)
129	$RO + O_2 \rightarrow$ carbonyl + $O_2{}^-$	[9.96×10^{-15}]	Wei et al. (2022)
130	$RO \rightarrow R$	[1.00×10^5 s^{-1}]	Campbell et al. (2023)
131	$RO_2 + AA \rightarrow ROOH + AA^\bullet$	[2.49×10^{-15}]	Buettner and Jurkiewicz (1996)
132	$RO_2 + DTT \rightarrow ROOH + DTT^\bullet$	[1.74×10^{-16}]	Campbell et al. (2023)
133	$RO_2 \rightarrow O_2{}^-$ + carbonyl	[10 s^{-1}]	Chevallier et al. (2004)
134	spin – trap + $RO \rightarrow$ spin – trap – RO	[2.11×10^{-18}]	Sueishi et al. (2014)
135	spin – trap + $OH \rightarrow$ spin – trap – OH	[1.66×10^{-12}]	Halliwell and Gutteridge (2015)
136	spin – trap + $O_2{}^- \rightarrow$ spin – trap – $O_2{}^-$	[1.99×10^{-21}]	Halliwell and Gutteridge (2015)
137	spin – trap + $R \rightarrow$ spin – trap – R	[3.98×10^{-15}]	Kemp (1999)

Table S2. Environmental input parameters for the different laboratory experiments

Experiment number	Temperature (K)	Citric acid (μM)	AA (μM)	UAH (μM)	GSH (μM)	DTT (μM)	Benzoate (mM)	Reference
1 – 10 (Fig. 3A, B)	298	300	200	100	100	0	0	Charrier et al. (2014)
11 – 12 (Fig. 3C)	298	300	200	100	100	0	10	Charrier and Anastasio (2015)
13 – 15 (Fig. 4A)	310	0	200	0	0	0	0	Expósito et al. (2024)
16 – 17 (Fig. 4B)	310	0	200	0	0	0	0	Shen et al. (2021)
18 – 21, 26 – 29 (Fig. 5A, D)	310	0	0	0	0	100	0	Charrier and Anastasio (2012)
22 – 23 (Fig. 5A, B)	310	0	0	0	0	50	0	Expósito et al. (2024)
24 – 25, 30 – 32 (Fig. 5C, E)	310	0	0	0	0	100	0	Xiong et al. (2017)

Table S3. Field data measurement for Grenoble site. Based on solubility measurements, the total Cu, Fe, and Mn concentrations were multiplied by 0.61, 0.017 and 0.54, respectively as input for the kinetic model. The metals are initialized as Cu(II), Fe(II), and Mn(II). SOA was determined using source apportionment outputs.

Date	1,4-NQN	1,2-NQN	9,10-PQN	Cu	Mn	Fe	Org	SOA	OP^{DTT}	OP^{AA}	PM10
	ng/m^3	ng/m^3	ng/m^3	ng/m^3	ng/m^3	ng/m^3	μg/m^3	μg/m^3	nmol/min/m^3	nmol/min/m^3	μg/m^3
1/2/2013	1.15E-03	6.52E-04	4.65E-04	4.76	1.55	104.99	6.33	0.17	1.26	1.63	10.94
1/5/2013	7.90E-03	7.55E-03	9.62E-03	16.69	21.19	492.40	14.87	0.67	3.68	4.81	27.19
1/8/2013	8.20E-03	6.64E-04	9.62E-03	24.60	23.62	669.13	18.77	0.94	5.55	5.51	38.17
1/11/2013	6.25E-03	1.73E-02	4.70E-04	12.57	7.93	246.16	11.12	1.10	3.05	3.66	18.33
1/14/2013	3.11E-03	6.59E-04	3.72E-04	4.64	3.11	163.72	6.38	0.28	1.34	1.28	16.51
1/17/2013	1.43E-02	1.27E-02	8.57E-03	19.04	16.30	665.03	14.60	0.76	4.61	2.26	43.81
1/20/2013	6.79E-03	9.03E-03	1.45E-02	5.00	4.08	146.46	9.84	1.06	2.13	2.11	20.88
1/23/2013	7.22E-03	6.58E-04	9.33E-02	27.69	20.62	612.05	20.50	1.09	6.42	7.23	36.35
1/26/2013	3.20E-02	6.65E-04	1.33E-01	30.80	9.80	427.00	20.93	3.37	7.85	6.24	44.07
1/29/2013	6.48E-03	5.53E-02	1.81E-03	33.10	12.14	631.00	16.66	0.55	5.41	5.99	30.50
2/1/2013	8.72E-03	1.36E-02	3.36E-02	29.72	26.84	763.87	20.57	1.30	5.81	6.23	31.70
2/4/2013	3.36E-03	6.67E-04	2.07E-03	13.69	5.13	257.12	13.05	0.43	3.83	3.95	23.98
2/7/2013	3.11E-03	6.62E-04	4.72E-04	5.62	2.43	107.39	3.83	0.13	1.52	0.90	9.72
2/10/2013	9.98E-03	6.65E-04	1.81E-01	5.69	3.37	164.51	12.27	2.31	2.90	2.51	20.96
2/13/2013	7.64E-03	1.03E-02	5.27E-03	4.47	3.39	113.52	12.49	1.06	3.46	1.59	31.57
2/16/2013	8.24E-03	6.64E-04	5.46E-02	16.87	13.74	415.06	18.89	1.21	4.72	4.61	32.93
2/19/2013	1.49E-02	6.68E-04	1.44E-01	24.46	16.26	557.67	20.70	1.73	6.18	5.07	38.90
2/22/2013	7.71E-03	6.63E-04	1.44E-02	8.82	7.91	256.76	10.47	0.84	3.81	1.67	36.47
2/25/2013	1.26E-02	6.67E-04	8.56E-03	9.32	6.96	225.89	18.19	2.06	4.04	2.11	49.69
2/28/2013	2.76E-02	6.60E-04	2.01E-01	50.33	24.70	745.89	30.14	1.83	11.40	6.76	72.24
3/3/2013	1.04E-02	1.43E-02	3.82E-02	16.84	9.32	461.91	23.19	1.70	7.18	4.29	60.19
3/6/2013	6.08E-03	6.44E-04	2.25E-03	23.01	12.23	588.70	14.93	0.36	3.04	3.63	34.00
3/9/2013	5.95E-03	6.52E-04	1.47E-02	12.59	10.88	301.49	11.58	0.91	2.11	2.58	27.00
3/12/2013	3.39E-03	6.52E-04	1.62E-04	7.87	3.48	182.10	5.03	0.44	1.77	1.16	9.85
3/15/2013	4.46E-03	7.14E-03	4.70E-04	7.20	5.01	222.44	5.91	0.26	2.45	0.81	18.85
3/18/2013	6.33E-03	1.12E-02	1.52E-03	26.41	5.32	230.79	7.12	0.61	2.85	2.81	16.71
3/21/2013	3.81E-03	6.52E-04	1.89E-03	23.39	10.97	367.35	7.84	0.31	2.96	2.65	14.61
3/24/2013	1.22E-02	1.04E-02	3.05E-02	7.69	5.04	199.45	12.42	0.24	4.04	0.93	42.18
3/27/2013	7.49E-03	6.52E-04	1.51E-02	17.14	8.80	500.76	13.03	0.68	4.95	1.76	32.76
3/30/2013	3.28E-03	1.16E-02	6.22E-03	5.34	6.07	150.39	6.10	0.27	1.80	1.22	10.52
4/3/2013	3.63E-03	7.61E-03	2.01E-03	13.21	7.32	340.34	11.35	0.76	3.74	1.44	33.59
4/5/2013	4.60E-03	6.52E-04	1.34E-02	12.31	9.11	343.78	11.62	0.87	4.78	1.63	46.21
4/8/2013	6.98E-03	6.52E-04	1.22E-02	14.81	7.24	418.06	12.54	0.86	4.77	1.92	39.24
4/11/2013	2.20E-03	6.52E-04	4.58E-04	6.71	11.71	249.43	6.91	0.40	1.63	0.91	12.25
4/14/2013	4.54E-03	6.52E-04	1.32E-04	9.18	3.81	244.23	8.91	0.71	1.85	1.01	15.12
4/17/2013	2.34E-03	9.13E-03	4.54E-04	16.89	12.49	603.94	13.08	0.19	3.71	1.51	27.77

Table S3. Continued

4/20/2013	3.38E-03	6.52E-04	4.66E-04	2.45	1.15	62.39	2.98	0.99	0.75	0.47	6.00
4/23/2013	5.01E-03	6.47E-03	4.58E-04	11.54	7.45	347.74	9.27	0.25	3.12	0.98	20.88
4/26/2013	2.54E-03	6.73E-03	1.87E-04	154.91	11.96	728.23	8.70	0.26	5.38	13.94	30.36
4/29/2013	6.68E-03	1.65E-02	4.63E-04	12.37	4.77	223.06	9.11	0.49	3.23	1.66	20.32
5/2/2013	1.92E-03	5.97E-03	1.29E-04	9.61	14.05	775.15	7.82	0.12	2.64	1.21	28.93
5/5/2013	1.24E-03	6.52E-04	4.61E-04	6.86	5.40	273.06	8.58	0.56	2.45	0.82	19.11
5/8/2013	1.67E-03	6.52E-04	4.49E-04	7.27	6.01	255.41	9.65	1.90	2.19	1.02	16.80
5/11/2013	1.83E-03	6.52E-04	4.74E-04	4.19	2.10	99.02	4.22	0.28	1.30	0.49	10.44
5/14/2013	6.33E-04	8.97E-03	4.50E-04	17.05	6.19	330.11	12.08	0.19	4.11	2.09	20.88
5/17/2013	1.02E-03	6.52E-04	4.57E-04	6.29	3.76	168.95	4.09	0.56	0.57	0.57	9.00
5/20/2013	8.95E-04	6.52E-04	4.54E-04	5.01	2.04	120.39	6.52	0.19	1.27	0.65	10.57
5/23/2013	2.18E-03	1.07E-02	4.58E-04	5.39	3.52	160.40	8.26	0.21	1.72	0.62	13.39
5/26/2013	2.33E-03	1.50E-03	4.61E-04	3.51	2.98	223.40	5.15	0.46	1.32	0.78	9.64
5/29/2013	1.31E-03	1.13E-02	1.46E-04	5.48	4.63	141.52	4.08	0.70	0.63	0.52	6.00
6/1/2013	1.32E-03	3.89E-02	4.60E-04	89.38	12.16	164.61	6.55	0.00	2.04	9.63	29.83
6/4/2013	9.96E-04	6.52E-04	4.52E-04	9.57	8.04	323.48	7.61	0.15	2.28	1.04	15.71
6/7/2013	1.16E-03	3.15E-02	1.16E-04	11.54	6.28	327.95	9.62	0.82	2.28	1.40	18.42
6/10/2013	1.44E-04	6.52E-04	4.53E-04	7.09	5.08	220.69	6.05	1.56	2.93	0.59	11.33
6/13/2013	5.68E-04	2.32E-02	4.53E-04	11.23	10.56	481.76	10.92	0.56	4.04	0.82	22.33
6/16/2013	1.31E-03	6.52E-04	4.49E-04	7.71	4.56	271.03	10.39	1.95	2.30	0.82	18.90
6/19/2013	1.34E-03	6.52E-04	4.47E-04	14.99	14.60	680.49	11.63	0.02	4.94	0.94	33.68
6/22/2013	4.06E-03	6.52E-04	4.48E-04	4.98	2.53	136.30	4.71	0.39	1.38	0.47	9.31
6/25/2013	7.66E-06	6.52E-04	4.56E-04	5.90	4.55	199.65	5.23	0.38	1.86	0.47	13.64
6/28/2013	4.56E-04	8.02E-03	4.56E-04	10.05	7.35	305.09	6.77	1.42	4.00	0.78	15.72
7/1/2013	2.99E-04	6.52E-04	3.02E-05	9.57	4.88	223.17	8.33	2.42	2.13	1.08	14.74
7/4/2013	7.63E-06	6.52E-04	4.54E-04	4.71	4.37	147.47	5.29	1.47	1.01	0.46	9.61
7/7/2013	2.32E-04	6.52E-04	4.46E-04	7.09	4.59	201.07	10.81	3.71	1.89	0.72	17.14
7/10/2013	7.73E-04	8.74E-02	4.50E-04	10.05	9.20	257.76	9.06	2.15	2.24	1.23	14.71
7/13/2013	3.74E-04	3.44E-02	4.53E-04	15.93	6.66	306.96	12.20	4.64	2.80	1.92	21.22
7/16/2013	2.42E-03	6.52E-04	4.46E-04	11.02	9.38	415.58	11.25	4.02	2.66	1.20	22.75
7/19/2013	5.15E-04	8.60E-03	4.55E-04	9.76	6.17	217.82	8.92	1.66	1.86	0.98	13.56
7/22/2013	7.57E-06	6.52E-04	4.51E-04	9.40	5.10	255.92	11.55	2.93	2.51	0.81	17.88
7/25/2013	3.40E-04	6.52E-04	4.46E-04	12.74	8.73	360.71	11.41	4.26	3.23	1.24	21.61
7/28/2013	7.47E-06	1.56E-02	4.45E-04	6.14	10.64	501.03	7.78	1.10	1.62	0.36	21.49
7/31/2013	2.61E-04	6.52E-04	4.45E-04	11.94	7.20	258.73	7.09	1.97	2.12	1.14	12.95
8/3/2013	9.41E-04	7.33E-03	4.46E-04	9.45	5.69	312.37	9.20	1.67	2.24	0.84	16.76
8/6/2013	5.14E-04	6.52E-04	4.44E-04	12.30	8.51	458.05	9.83	3.33	3.10	1.05	23.34
8/9/2013	2.40E-04	6.52E-04	4.54E-04	5.54	2.32	130.61	5.61	2.08	1.46	0.43	10.10
8/12/2013	3.96E-04	5.96E-03	4.46E-04	8.94	3.74	220.11	6.42	1.96	1.71	0.90	11.90
8/15/2013	2.39E-03	2.68E-02	2.86E-05	7.75	4.45	215.97	8.56	2.71	2.03	0.91	15.38
8/18/2013	9.23E-04	5.15E-02	4.46E-04	21.28	3.47	193.62	9.80	3.97	3.16	2.53	16.41

Table S3. Continued

8/21/2013	9.66E-04	6.52E-04	4.54E-04	18.63	6.10	278.15	7.09	3.44	2.88	2.27	14.53
8/24/2013	2.72E-04	6.39E-04	4.56E-04	8.85	4.14	218.05	7.32	2.72	1.78	0.95	14.01
8/27/2013	6.51E-04	6.43E-04	3.85E-04	9.90	4.22	208.92	4.86	1.68	1.78	1.04	10.31
8/30/2013	1.04E-03	6.31E-04	3.92E-04	12.89	10.28	337.62	8.50	3.44	2.76	1.39	18.55
9/2/2013	3.54E-04	6.35E-04	4.53E-04	9.57	6.36	276.60	5.44	0.93	2.52	1.30	15.19
9/5/2013	5.44E-03	6.26E-04	1.51E-03	87.90	12.05	594.62	10.59	3.81	5.94	9.04	23.77
9/8/2013	7.65E-06	6.37E-04	4.55E-04	21.98	11.30	425.65	9.57	0.47	0.67	0.34	9.00
9/11/2013	7.45E-04	6.44E-04	4.60E-04	6.90	4.23	185.81	3.73	0.84	1.05	0.57	11.00
9/14/2013	1.71E-03	6.37E-04	9.29E-04	10.27	4.66	245.15	5.30	1.14	1.95	1.31	9.29
9/17/2013	2.36E-03	6.59E-04	4.62E-04	7.80	3.50	185.15	3.12	0.32	1.31	0.91	9.33
9/20/2013	7.37E-04	4.18E-03	4.52E-04	8.52	4.90	240.33	3.50	0.18	2.27	0.98	8.06
9/23/2013	2.23E-03	6.34E-04	4.53E-04	33.39	13.89	697.07	10.13	2.49	2.80	1.54	25.00
9/26/2013	7.22E-03	1.56E-02	5.58E-03	18.07	13.38	547.86	9.69	0.69	5.29	5.42	37.00
9/29/2013	1.87E-03	6.37E-04	4.55E-04	9.98	4.40	263.65	6.73	0.47	2.33	1.53	13.24
10/2/2013	1.94E-03	6.36E-04	4.54E-04	18.73	18.51	499.49	8.32	0.19	2.88	1.47	16.03
10/5/2013	1.10E-03	6.40E-04	4.57E-04	5.92	2.41	129.81	3.84	0.30	0.56	0.36	6.00
10/8/2013	1.99E-03	6.39E-04	2.59E-04	6.50	2.07	143.41	3.29	0.43	1.53	0.78	21.00
10/11/2013	1.25E-03	6.47E-04	4.62E-04	29.92	8.12	361.41	7.46	0.16	3.12	2.43	15.45
10/14/2013	2.75E-03	1.57E-02	1.30E-03	20.96	7.36	416.78	9.91	0.25	2.83	2.64	15.57
10/17/2013	1.70E-03	6.94E-04	4.96E-04	14.11	10.14	326.22	5.87	0.28	1.79	1.08	11.00
10/20/2013	2.45E-03	6.46E-04	1.37E-03	8.49	3.92	241.78	7.12	0.13	1.73	0.78	11.87
10/23/2013	1.92E-03	3.91E-02	5.09E-03	8.68	9.62	333.02	4.08	0.28	1.57	0.49	11.66
10/26/2013	3.38E-03	6.48E-04	5.18E-03	24.09	25.96	618.78	9.20	0.14	3.47	1.78	22.00
10/29/2013	1.59E-03	6.43E-04	2.21E-03	9.70	7.20	221.41	3.09	0.38	1.15	0.81	8.00
11/1/2013	4.94E-03	6.47E-04	2.43E-02	26.92	12.40	567.66	11.61	0.25	4.12	3.09	22.01
11/4/2013	2.19E-03	6.52E-04	3.10E-02	7.53	3.74	190.63	5.72	0.40	1.40	1.72	8.70
11/7/2013	4.97E-03	4.15E-02	1.04E-02	37.48	10.43	662.97	9.35	0.26	3.62	3.96	17.38
11/13/2013	3.33E-02	6.52E-04	5.73E-05	44.28	19.02	752.37	16.33	0.00	4.61	2.89	34.83
11/16/2013	1.59E-02	6.52E-04	3.39E-02	15.39	14.29	395.20	10.77	1.06	3.21	1.41	26.94
11/19/2013	3.27E-03	6.52E-04	2.37E-03	8.42	4.98	191.44	7.47	0.00	2.05	0.91	14.12
11/22/2013	9.24E-03	6.52E-04	5.62E-03	3.88	1.60	91.13	4.08	0.55	1.46	1.63	7.74
11/28/2013	2.99E-02	6.52E-04	4.79E-04	25.87	29.94	615.46	16.47	0.00	2.90	1.72	39.74
12/1/2013	1.12E-02	6.52E-04	1.93E-03	8.82	5.78	240.97	10.95	0.23	2.28	1.74	25.13
12/4/2013	1.36E-02	1.88E-03	7.88E-02	46.20	23.94	939.80	23.52	1.38	6.83	5.88	41.01
12/7/2013	1.27E-02	6.52E-04	1.83E-01	19.14	11.15	439.25	13.47	4.24	2.86	3.01	25.74
12/10/2013	4.07E-02	4.27E-03	1.26E-01	169.70	40.43	1259.02	27.35	8.83	10.34	16.19	48.12
12/13/2013	3.36E-02	1.53E-02	3.79E-01	58.03	41.92	1375.40	31.27	16.64	8.21	8.48	53.94
12/16/2013	3.82E-02	4.52E-02	1.75E-01	63.07	25.99	1502.18	31.51	11.58	9.74	8.34	57.40
12/19/2013	1.64E-02	6.52E-04	2.11E-02	9.75	16.85	254.15	6.77	1.22	1.76	1.37	12.61
12/22/2013	1.58E-02	6.52E-04	5.58E-02	6.36	7.41	134.25	6.03	0.02	1.42	1.78	11.56
12/25/2013	4.58E-03	6.52E-04	4.59E-04	1.51	1.77	30.54	3.94	0.59	0.67	0.26	7.40
12/31/2013	1.91E-02	6.52E-04	1.71E-01	30.28	7.11	584.12	13.77	3.27	4.11	4.13	22.32

Table S4. Field data measurement for Paris site. Based on solubility measurements, the total Cu, Fe, and Mn concentrations were multiplied by 0.77, 0.061 and 0.95, respectively as input for the kinetic model. The metals are initialized as Cu(II), Fe(II), and Mn(II). SOA was determined using source apportionment outputs.

Date	1,4-NQN	1,2-NQN	9,10-PQN	Cu	Mn	Fe	Org	SOA	OP^{DTT}	OP^{AA}	PM10
	ng/m^3	ng/m^3	ng/m^3	ng/m^3	ng/m^3	ng/m^3	$\mu g/m^3$	$\mu g/m^3$	$nmol/min/m^3$	$nmol/min/m^3$	$\mu g/m^3$
06/03/2015 15:00:00	0.22	0.19	0.37	10.54	0.62	217.40	7.22	2.37	2.02	1.57	30.62
06/03/2015 19:00:00	0.21	0.00	0.45	9.46	14.00	318.92	9.98	9.81	2.83	3.95	32.49
06/03/2015 23:00:00	0.14	0.41	0.52	2.12	6.93	104.99	8.16	3.43	1.74	2.63	32.15
07/03/2015 03:00:00	0.26	0.25	0.92	4.39	9.74	187.13	9.82	7.15	2.89	3.11	34.23
07/03/2015 07:00:00	0.16	0.00	0.46	8.10	2.95	143.99	10.39	4.57	3.91	2.29	35.98
07/03/2015 11:00:00	0.17	0.08	0.35	4.47	6.03	119.92	8.43	1.89	1.90	0.57	23.72
07/03/2015 15:00:00	0.24	0.21	0.37	6.38	8.99	210.31	12.39	6.30	2.72	1.46	26.61
07/03/2015 19:00:00	0.23	0.31	0.47	8.65	6.52	164.30	23.35	7.13	3.36	3.61	30.26
07/03/2015 23:00:00	0.15	0.38	0.55	12.49	13.23	279.13	17.59	6.43	3.91	2.99	33.22
08/03/2015 03:00:00	0.20	0.53	0.59	5.23	16.03	227.84	14.55	5.78	1.92	2.45	32.93
08/03/2015 07:00:00	0.23	0.53	0.41	9.29	12.08	201.23	11.44	3.33	1.09	0.75	27.55
08/03/2015 11:00:00	0.26	0.14	0.34	12.48	7.99	244.09	7.51	0.94	0.85	1.34	18.37
08/03/2015 15:00:00	0.21	0.16	0.33	9.05	8.54	258.30	8.70	0.91	1.28	1.20	12.30
08/03/2015 19:00:00	0.11	0.26	0.37	10.92	8.90	313.76	13.38	2.04	2.46	1.11	29.09
08/03/2015 23:00:00	0.04	0.00	0.34	5.05	3.95	168.93	2.25	0.51	0.83	0.65	14.84
09/03/2015 03:00:00	0.04	0.01	0.34	7.16	5.60	219.54	2.17	0.77	1.08	0.80	12.58
09/03/2015 07:00:00	0.03	0.00	0.34	8.61	6.12	289.01	4.67	2.16	2.10	1.06	21.81
09/03/2015 11:00:00	0.12	0.00	0.34	9.16	6.88	334.03	6.24	1.23	2.45	0.22	27.21
09/03/2015 15:00:00	0.10	0.19	0.37	11.80	9.51	345.43	8.33	1.96	1.80	2.05	25.76
09/03/2015 19:00:00	0.04	0.04	0.39	7.46	7.97	271.65	8.45	2.74	2.75	2.29	30.86
09/03/2015 23:00:00	0.07	0.15	0.58	6.13	6.69	268.96	9.38	4.55	1.07	3.00	34.35
10/03/2015 03:00:00	0.04	0.00	0.59	8.26	6.29	266.37	12.67	4.28	3.11	3.54	37.30
10/03/2015 07:00:00	0.05	0.00	0.42	17.06	9.20	462.00	11.35	4.88	3.86	2.87	38.79
10/03/2015 11:00:00	0.02	0.00	0.34	10.42	8.01	347.54	7.28	0.69	2.44	1.73	33.25
10/03/2015 15:00:00	0.02	0.00	0.35	22.02	16.38	600.34	8.29	1.49	3.35	2.21	24.16
10/03/2015 19:00:00	0.03	0.00	0.37	48.52	24.64	1087.24	13.66	2.39	6.13	5.91	35.05
10/03/2015 23:00:00	0.04	0.04	0.74	11.73	18.77	545.84	8.27	3.63	4.18	2.08	35.16
11/03/2015 03:00:00	0.04	0.00	0.89	15.60	20.41	609.16	7.96	5.24	2.60	2.15	37.24
11/03/2015 07:00:00	0.03	0.00	0.42	24.26	21.04	842.97	11.95	3.28	5.29	2.42	53.79
11/03/2015 11:00:00	0.09	0.00	0.35	9.00	15.85	466.22	6.41	2.79	2.43	1.77	53.89
11/03/2015 15:00:00	0.04	0.00	0.33	22.89	24.79	750.05	11.18	2.99	4.71	1.94	48.75
11/03/2015 19:00:00	0.07	0.00	0.39	22.66	20.95	723.48	12.31	5.75	5.84	4.14	51.67
11/03/2015 23:00:00	0.07	0.14	0.45	10.83	21.60	449.98	9.41	3.65	3.96	2.71	41.52
12/03/2015 03:00:00	0.08	0.00	0.57	15.33	20.50	611.86	9.78	3.92	3.02	2.91	30.12
12/03/2015 07:00:00	0.08	0.00	0.43	19.50	24.11	675.57	11.22	2.44	3.95	2.46	33.22
12/03/2015 11:00:00	0.07	0.00	0.34	9.36	17.14	403.50	7.63	1.39	2.54	1.53	24.45
12/03/2015 15:00:00	0.14	0.00	0.35	10.30	17.45	412.96	6.12	1.93	2.05	1.24	24.48

Table S4. Continued

12/03/2015 19:00:00	0.11	0.00	0.37	10.42	18.69	432.01	7.90	2.33	2.50	1.74	24.90
12/03/2015 23:00:00	0.29	0.08	0.50	6.71	8.30	288.74	6.33	3.13	1.73	1.16	21.41
13/03/2015 03:00:00	0.13	0.00	0.51	8.10	9.94	349.97	6.98	2.93	2.31	1.15	25.83
13/03/2015 07:00:00	0.11	0.00	0.42	22.17	16.99	737.17	11.43	3.46	4.87	2.38	36.75
13/03/2015 11:00:00	0.16	0.00	0.36	13.80	12.67	533.46	8.78	2.91	3.98	1.25	37.27
13/03/2015 15:00:00	0.14	0.00	0.36	13.66	11.49	516.52	7.86	3.14	3.40	1.45	31.57
13/03/2015 19:00:00	0.17	0.00	0.53	27.37	15.98	840.54	14.14	9.39	5.88	3.83	37.61
13/03/2015 23:00:00	0.15	0.00	1.20	17.47	13.33	567.06	15.98	13.82	5.65	2.93	46.38
14/03/2015 03:00:00	0.07	0.00	1.01	10.88	12.70	422.62	10.12	4.80	2.87	1.32	41.04
14/03/2015 07:00:00	0.15	0.04	0.66	12.05	12.03	450.65	8.71	3.56	3.63	0.94	36.39
14/03/2015 11:00:00	0.14	0.00	0.35	9.99	21.28	957.88	8.85	2.40	1.90	1.09	46.01
14/03/2015 15:00:00	0.08	0.00	0.36	12.40	21.28	963.64	11.18	2.99	5.54	1.22	58.71
14/03/2015 19:00:00	0.13	0.00	0.50	9.80	13.20	462.13	14.54	5.28	3.75	0.73	47.78
14/03/2015 23:00:00	0.07	0.00	0.42	9.18	11.13	345.23	13.21	2.14	5.25	1.20	65.75
15/03/2015 03:00:00	0.07	0.00	0.50	7.48	9.05	303.95	11.93	3.21	3.36	1.89	65.22
15/03/2015 07:00:00	0.15	0.00	0.42	9.24	9.60	351.21	11.46	4.00	4.63	1.78	54.73
15/03/2015 11:00:00	0.18	0.00	0.36	10.63	7.54	334.65	9.75	3.65	5.43	1.68	48.18
15/03/2015 15:00:00	0.16	0.38	0.34	11.08	8.64	381.66	10.15	3.07	2.31	2.36	33.15
15/03/2015 19:00:00	0.06	0.00	0.34	15.03	7.41	338.13	11.66	2.83	2.44	3.54	27.97
15/03/2015 23:00:00	0.08	0.00	0.45	8.96	7.82	268.27	10.67	3.62	1.68	3.58	29.07
16/03/2015 03:00:00	0.05	0.00	0.41	13.98	11.22	442.16	11.44	2.28	2.62	3.67	29.38
16/03/2015 07:00:00	0.17	0.00	0.39	31.25	21.26	992.28	16.57	5.36	5.22	2.89	46.86
16/03/2015 11:00:00	0.11	0.00	0.34	19.29	13.80	606.56	13.90	2.38	4.60	1.70	54.93
16/03/2015 15:00:00	0.47	0.00	0.34	24.43	19.34	1077.52	16.64	4.12	5.18	4.15	54.91
16/03/2015 19:00:00	0.41	0.62	0.39	17.30	14.11	602.94	18.48	7.60	4.34	4.00	59.57
16/03/2015 23:00:00	0.07	0.02	0.47	11.58	12.68	489.62	19.39	6.85	4.44	3.77	70.05
17/03/2015 03:00:00	0.04	0.00	0.46	12.89	14.74	488.04	20.64	6.27	4.55	3.60	75.55
17/03/2015 07:00:00	0.10	0.00	0.46	30.80	24.47	1156.53	22.99	9.18	10.07	3.83	87.09
17/03/2015 11:00:00	0.07	0.00	0.33	20.87	15.65	730.31	12.33	1.59	4.49	1.94	37.95
17/03/2015 15:00:00	0.16	0.00	0.34	40.50	24.39	1323.60	17.41	2.59	7.79	2.91	52.34
17/03/2015 19:00:00	0.28	0.64	0.40	36.47	18.03	1067.22	21.37	6.93	7.71	4.19	61.57
17/03/2015 23:00:00	0.11	0.11	0.57	19.02	15.45	681.70	20.44	7.21	7.63	4.15	63.50
18/03/2015 03:00:00	0.15	0.32	0.48	19.37	19.79	744.07	20.46	8.94	6.91	3.94	70.33
18/03/2015 07:00:00	0.04	0.00	0.37	28.62	28.24	1254.23	25.10	6.47	13.69	4.83	113.18
18/03/2015 11:00:00	0.04	0.00	0.34	21.52	24.02	1007.76	21.39	4.93	11.08	2.60	108.70
18/03/2015 15:00:00	0.23	0.00	0.35	19.01	23.72	947.83	19.51	5.54	8.76	2.72	113.10
18/03/2015 19:00:00	0.04	0.00	0.35	13.07	15.09	549.47	16.14	2.60	5.93	4.83	104.96
18/03/2015 23:00:00	0.14	0.00	0.37	7.87	8.14	302.61	9.44	2.62	3.55	2.30	59.77
19/03/2015 03:00:00	0.11	0.00	0.35	6.36	8.51	278.36	8.02	1.75	2.76	2.18	56.41
19/03/2015 07:00:00	0.12	0.00	0.34	14.02	15.36	733.30	10.56	0.88	3.76	1.43	56.58
19/03/2015 11:00:00	0.04	0.00	0.34	9.31	18.49	844.69	9.92	2.03	5.99	2.78	45.95

Table S4. Continued

19/03/2015 15:00:00	0.06	0.00	0.34	13.28	11.11	493.02	9.27	1.02	2.03	0.39	37.10
19/03/2015 19:00:00	0.12	0.00	0.35	11.53	9.59	404.57	11.09	2.34	4.49	2.39	42.57
19/03/2015 23:00:00	0.10	0.00	0.38	8.26	10.49	394.09	12.10	2.78	4.56	1.12	76.78
20/03/2015 03:00:00	0.05	0.07	0.34	14.37	13.00	504.11	12.55	2.05	10.12	3.28	89.66
20/03/2015 07:00:00	0.03	0.00	0.35	23.03	22.22	1057.58	17.72	1.55	11.98	2.92	111.29
20/03/2015 11:00:00	0.12	0.00	0.35	22.75	22.40	1032.53	23.25	2.45	11.53	2.27	121.51
20/03/2015 15:00:00	0.06	0.00	0.34	23.38	22.55	1037.96	19.89	3.36	14.83	3.37	115.67
20/03/2015 19:00:00	0.05	0.00	0.37	21.74	19.39	892.14	23.80	5.89	15.18	3.96	120.07
20/03/2015 23:00:00	0.05	0.00	0.34	16.64	15.92	668.41	23.16	3.13	13.09	3.60	121.08
21/03/2015 03:00:00	0.03	0.00	0.38	10.14	12.15	419.70	19.04	4.59	11.62	2.02	130.00
21/03/2015 07:00:00	0.05	0.00	0.34	8.12	8.12	303.86	11.82	2.75	7.35	0.84	77.09
21/03/2015 11:00:00	0.11	0.00	0.36	7.04	13.45	330.20	7.77	1.95	6.68	1.33	54.68
21/03/2015 15:00:00	0.04	0.00	0.33	5.04	11.18	259.42	3.49	0.39	1.00	0.48	13.79
21/03/2015 19:00:00	0.04	0.00	0.35	6.27	7.63	203.14	3.80	0.82	1.83	1.09	13.49

Table S5. Field data measurement for London site in the summer. As soluble fractions of the metals were not measured, we use median values of the soluble metal fraction as determined from field measurement studies ((Connell et al., 2006; Manousakas et al., 2014; Heal et al., 2005; Giorio et al., 2025)). The metals are initialized as Cu(II), Fe(II), and Mn(II). Org was determined using PM composition data.

date	Cu	Mn	Fe	Org	OP^{DHA}	PM2.5
	$\mu g/m^3$	$\mu g/m^3$	$\mu g/m^3$	$\mu g/m^3$	$nmol/m^3$	$\mu g/m^3$
23.05.2023 05:00	0.00146	2.00E-05	0.05924	2.05339	5.84	6.36368
23.05.2023 06:00	0.00209	5.00E-05	0.08393	1.76607	5.48	6.63467
23.05.2023 07:00	0.0082	5.60E-04	0.22657	1.7379	5.84	6.88302
23.05.2023 08:00	0.01431	0.00108	0.36921	1.78526	7.04	6.40472
23.05.2023 20:00	0.00545	3.00E-04	0.21892	6.23438	8.84	10.4316
23.05.2023 21:00	0.00572	2.40E-04	0.21208	6.0377	15.36	8.56321
23.05.2023 22:00	0.00599	1.90E-04	0.20523	4.28657	15.72	7.56863
23.05.2023 23:00	0.00612	1.80E-04	0.23616	3.95701	16.72	8.11297
24.05.2023 00:00	0.00625	1.70E-04	0.26709	3.81611	18.08	7.45566
24.05.2023 01:00	0.00604	4.70E-04	0.26585	2.6935	19.52	6.46462
24.05.2023 02:00	0.00584	7.70E-04	0.2646	3.15452	18.68	8.14387
24.05.2023 03:00	0.00577	7.10E-04	0.23611	4.09349	19.08	8.64929
24.05.2023 04:00	0.0057	6.50E-04	0.20762	4.85919	16.4	9.7842
24.05.2023 05:00	0.00437	5.40E-04	0.18987	4.2674	16.96	10.86085
24.05.2023 06:00	0.00304	4.40E-04	0.17212	3.08327	16.12	10.8184
24.05.2023 07:00	0.00281	6.30E-04	0.17188	2.97031	17	10.25472
24.05.2023 08:00	0.00258	8.30E-04	0.17164	3.29615	12.64	9.93137
24.05.2023 09:00	0.00258	5.30E-04	0.13917	2.79669	4.4	9.43608
24.05.2023 13:00	0.00218	2.30E-04	0.09569	5.14333	5.2	9.73349
26.05.2023 18:00	0.00687	8.40E-04	0.25632	3.86228	5.68	11.6816
31.05.2023 14:00	0.00195	2.00E-05	0.07723	3.11249	12.88	7.6842
31.05.2023 15:00	0.00154	1.00E-05	0.06422	3.05584	5.76	7.94646
03.06.2023 15:00	0.00158	1.00E-05	0.08398	4.29253	7.76	7.02972
03.06.2023 16:00	0.00175	1.00E-05	0.08596	4.62102	4.28	6.95731
04.06.2023 18:00	0.00332	1.00E-04	0.18375	4.68414	6.4	6.8783
04.06.2023 19:00	0.00438	5.70E-04	0.21497	4.89139	9.36	7.61958
04.06.2023 20:00	0.00545	0.00105	0.24618	4.25398	6.64	7.40189
05.06.2023 09:00	0.00604	2.00E-04	0.15008	1.55145	4.04	5.2533
07.06.2023 17:00	0.00615	0.00123	0.2257	4.91407	8.32	10.75236
07.06.2023 18:00	0.00632	9.60E-04	0.23672	5.50042	7.52	11.76651

Table S5. Continued

07.06.2023 19:00	0.00584	0.00107	0.25252	5.29289	9.08	11.90802
07.06.2023 20:00	0.00535	0.00118	0.26833	4.86379	9.76	11.64151
07.06.2023 21:00	0.00343	5.90E-04	0.16813	3.39017	10.04	9.31179
08.06.2023 09:00	0.00249	9.00E-05	0.098	2.21778	4.16	8.32689
08.06.2023 11:00	0.00217	1.00E-05	0.08025	3.64314	5.36	8.83962
10.06.2023 17:00	0.00649	0.00171	0.24954	15.23334	6.2	18.83255
10.06.2023 18:00	0.00587	0.0013	0.24805	15.00493	5.96	17.96934
11.06.2023 16:00	0.00892	0.00232	0.33402	15.18721	7.12	20.19104
11.06.2023 17:00	0.00952	0.00629	0.34315	17.84065	4.4	20.61085
11.06.2023 18:00	0.01012	0.01027	0.35228	21.89867	11.44	24.5566
11.06.2023 21:00	0.01267	0.00319	0.46508	19.56444	12.48	28.63679
11.06.2023 22:00	0.0069	0.00227	0.34345	18.61022	13.6	31.67925
11.06.2023 23:00	0.00489	0.00113	0.23958	18.10934	14.2	30.37264
12.06.2023 01:00	0.00528	8.00E-04	0.21436	16.84179	9.04	27.14387
12.06.2023 02:00	0.00767	0.0016	0.29299	19.86018	4.16	28.89387
12.06.2023 08:00	0.01808	0.00328	0.49112	15.44187	8.52	27.44575
12.06.2023 09:00	0.01951	0.0027	0.45669	14.41594	8.52	21.70755
17.06.2023 16:00	0.00698	0.00329	0.26615	11.79703	5.04	16.21462
17.06.2023 17:00	0.00819	0.00348	0.32612	10.84835	5.28	16.1816
17.06.2023 18:00	0.0094	0.00367	0.3861	11.11287	4.56	15.59906
17.06.2023 19:00	0.00843	0.00351	0.36726	11.466	4.28	17.26651
17.06.2023 20:00	0.00746	0.00336	0.34843	11.89539	4.24	21.1533
17.06.2023 21:00	0.00613	0.00249	0.30307	12.10355	4.08	21.16745
20.06.2023 16:00	0.00554	6.10E-04	0.22294	6.25424	4.24	5.78137
20.06.2023 18:00	0.00735	6.10E-04	0.31783	8.65386	5.16	5.81392
20.06.2023 19:00	0.00726	4.60E-04	0.31521	8.80862	6.08	6.01014
20.06.2023 20:00	0.00716	3.20E-04	0.31259	10.37676	5.24	6.42925
20.06.2023 21:00	0.00671	3.60E-04	0.28148	8.76427	5	6.42311
23.06.2023 01:00	0.00534	5.60E-04	0.27103	4.88142	5.76	5.11085
23.06.2023 02:00	0.00461	6.00E-04	0.23803	4.72821	4.72	5.02358
24.06.2023 01:00	0.00482	1.60E-04	0.22619	5.16224	4.36	7.38255
27.06.2023 14:00	0.00659	7.90E-04	0.22216	5.03987	4.32	6.9717
27.06.2023 16:00	0.00816	7.50E-04	0.26471	5.18595	4.36	7.91934
27.06.2023 18:00	0.00723	6.50E-04	0.29629	8.83731	5.52	10.74057
02.07.2023 01:00	0.00448	9.20E-04	0.11277	8.66384	5.48	19.6934
02.07.2023 02:00	0.00393	5.30E-04	0.12182	8.40271	4.44	18.47406
02.07.2023 13:00	0.00448	5.00E-04	0.22417	3.70091	4.44	7.46887
02.07.2023 14:00	0.00395	5.10E-04	0.20924	3.34075	5.52	8.36604
02.07.2023 15:00	0.00341	5.20E-04	0.19431	3.24729	4.2	7.90943
02.07.2023 17:00	0.00239	2.50E-04	0.1989	3.5743	5.96	7.88656
02.07.2023 18:00	0.00378	3.80E-04	0.2097	4.75476	7.04	8.05519
02.07.2023 19:00	0.00518	5.00E-04	0.22049	4.12646	6.48	7.4941

Table S5. Continued

02.07.2023 21:00	0.00606	5.00E-04	0.27883	3.21587	4.16	8.42618
04.07.2023 11:00	0.00629	3.30E-04	0.20777	5.72633	5.76	8.375
04.07.2023 12:00	0.00613	0.00167	0.21938	7.69142	9.92	10.06604
04.07.2023 13:00	0.00598	0.00301	0.23099	7.67072	8.28	11.28514
04.07.2023 14:00	0.00668	0.00169	0.23535	8.90546	8.48	12.15802
04.07.2023 15:00	0.00738	3.60E-04	0.23971	8.38157	9.2	11.04953
04.07.2023 16:00	0.00647	2.90E-04	0.21152	7.82144	7.16	9.97406
04.07.2023 17:00	0.00556	2.20E-04	0.18333	8.37361	6	10.88208
04.07.2023 18:00	0.00685	0.00131	0.31827	11.02169	4.12	9.40047
05.07.2023 01:00	0.00187	4.00E-05	0.0822	3.16805	4.48	5.5158
05.07.2023 02:00	0.00219	2.00E-05	0.08787	2.6562	6.6	5.73774
13.07.2023 15:00	0.0048	2.60E-04	0.17916	1.72116	6.36	6.33396
13.07.2023 16:00	0.00655	6.20E-04	0.24277	1.80411	4.24	6.48278
13.07.2023 17:00	0.0083	9.90E-04	0.30637	1.80486	4.04	5.82524
15.07.2023 18:00	0.0038	6.00E-05	0.13358	1.30839	4.68	11.1533
15.07.2023 19:00	0.00351	9.00E-05	0.13199	1.61196	6.44	13.12972
16.07.2023 17:00	0.0058	6.00E-05	0.17716	1.49688	5.96	5.75896
16.07.2023 18:00	0.00509	2.40E-04	0.17431	1.64284	5.08	7.08679
16.07.2023 19:00	0.00438	4.30E-04	0.17145	1.51388	10.96	7.25991
16.07.2023 21:00	0.00471	2.20E-04	0.17922	1.69114	5.12	7.36392
16.07.2023 22:00	0.00441	1.40E-04	0.17959	1.11696	5.64	5.91014
16.07.2023 23:00	0.00412	7.00E-05	0.17996	1.08488	5	6.55708
17.07.2023 02:00	0.00247	7.00E-05	0.1029	0.62433	7.04	5.59481
17.07.2023 03:00	0.00276	1.30E-04	0.12748	0.49247	15.68	5.6908
17.07.2023 06:00	0.00707	6.20E-04	0.2633	0.65547	6.48	6.97453
17.07.2023 07:00	0.00835	0.00123	0.31621	0.7043	10.36	6.05755
17.07.2023 08:00	0.00575	8.20E-04	0.25223	0.8174	10.76	5.15165
18.07.2023 17:00	0.00963	0.00105	0.33391	1.17878	5.12	5.61887
18.07.2023 18:00	0.00889	0.00109	0.30192	1.54693	4.8	6.01557
25.07.2023 05:00	0.00828	0.00234	0.47093	0.58967	9.56	5.09552
25.07.2023 06:00	0.00885	0.00286	0.52276	1.04132	8.72	6.89906
25.07.2023 07:00	0.00942	0.00339	0.57459	1.04418	7.44	6.74552
25.07.2023 08:00	0.00618	0.00249	0.4584	0.75678	6.28	5.26958
05.08.2023 02:00	0.00643	4.70E-04	0.23692	1.37928	8.8	7.91274
05.08.2023 03:00	0.00597	3.10E-04	0.19787	1.36016	7.32	8.06462
05.08.2023 04:00	0.00561	4.80E-04	0.17711	1.14999	5.68	8.74057
05.08.2023 05:00	0.00526	6.50E-04	0.15635	0.96636	5.2	9.29858
05.08.2023 06:00	0.0055	4.70E-04	0.15695	1.04361	4.44	10.73821
14.08.2023 10:00	0.00524	3.40E-04	0.15825	1.13802	7.52	6.70448
14.08.2023 18:00	0.00878	0.00128	0.24241	1.32291	17.64	5.03585
14.08.2023 20:00	0.00458	1.20E-04	0.20256	2.45287	19.24	5.72807
15.08.2023 18:00	0.00852	4.20E-04	0.24634	2.32305	15.16	6.48538

Table S5. Continued

15.08.2023 20:00	0.00576	4.60E-04	0.21859	3.30527	9.68	7.60684
15.08.2023 22:00	0.00672	0.00196	0.43329	1.87244	10.96	5.86981
16.08.2023 20:00	0.00504	0.00379	0.25237	1.26522	9.88	6.83137
16.08.2023 22:00	0.00349	0.00109	0.21292	1.64547	5.8	9.50448
17.08.2023 13:00	0.00475	2.80E-04	0.16476	0.98544	4.88	5.91958
17.08.2023 14:00	0.00401	3.00E-05	0.14049	1.226	6.88	5.44033
17.08.2023 18:00	0.00663	7.60E-04	0.2608	1.08627	10.52	5.16038
17.08.2023 19:00	0.00562	6.20E-04	0.22449	0.81358	9.32	5.22453
17.08.2023 20:00	0.0046	4.70E-04	0.18818	1.1005	9.08	6.56321
17.08.2023 21:00	0.00385	2.60E-04	0.17093	0.84524	7.64	7.72193
17.08.2023 22:00	0.0031	4.00E-05	0.15367	0.8459	4.44	7.65142
18.08.2023 01:00	0.00211	1.00E-05	0.09726	0.66439	4	8.16486
18.08.2023 16:00	0.00734	0.00184	0.26693	2.34348	16.72	24.82547
18.08.2023 17:00	0.00838	0.00328	0.31657	2.5194	18.16	30.8066
18.08.2023 18:00	0.00942	0.00473	0.36621	2.95657	17.88	34.48585
18.08.2023 19:00	0.00784	0.00339	0.33482	3.51145	15.44	34.37028
18.08.2023 20:00	0.00626	0.00205	0.30343	3.09941	17.64	33.33962
18.08.2023 21:00	0.0062	0.00183	0.28084	3.23171	13.6	32.45519
18.08.2023 22:00	0.00613	0.00161	0.25825	3.03763	8.8	30.07311
19.08.2023 01:00	0.00383	3.80E-04	0.19397	1.66026	4.12	8.13939
19.08.2023 11:00	0.0053	1.70E-04	0.18714	1.08603	4.48	6.61179
19.08.2023 20:00	0.00687	4.50E-04	0.2634	2.17863	5.8	7.83892
19.08.2023 21:00	0.00714	5.10E-04	0.27348	2.24588	10.84	8.14481
19.08.2023 22:00	0.00741	5.60E-04	0.28356	1.48206	10.84	6.67099
20.08.2023 18:00	0.00595	4.20E-04	0.23588	1.6371	11.72	5.22382
20.08.2023 19:00	0.00635	4.70E-04	0.25133	2.49115	11.64	7.22783
20.08.2023 20:00	0.00676	5.20E-04	0.26678	3.11171	9.72	7.62453
20.08.2023 21:00	0.00706	4.60E-04	0.27062	1.91077	10.92	5.82995
20.08.2023 22:00	0.00735	4.10E-04	0.27446	1.48903	8	6.41533
21.08.2023 16:00	0.00609	3.00E-05	0.19136	1.37617	16.12	6.03632
21.08.2023 17:00	0.00603	2.00E-05	0.2144	1.42735	18.44	6.19788
21.08.2023 19:00	0.00501	9.00E-05	0.20903	2.02887	24.44	6.72264
21.08.2023 20:00	0.00406	1.90E-04	0.18061	2.23245	23.88	6.78514
22.08.2023 22:00	0.00884	0.00217	0.43442	1.11544	35.04	5.07193
23.08.2023 03:00	0.00614	6.80E-04	0.12816	0.9027	29.76	7.49222
23.08.2023 04:00	0.0063	0.00123	0.1594	1.1996	34.16	6.1842
23.08.2023 05:00	0.00859	0.00264	0.38608	1.09321	37.04	6.86368
23.08.2023 06:00	0.01087	0.00405	0.61275	1.27363	29.72	7.09528
23.08.2023 07:00	0.01033	0.00377	0.59167	0.96414	29.36	6.81392
23.08.2023 08:00	0.00979	0.00349	0.57058	0.85327	31.64	6.18844
23.08.2023 18:00	0.01218	0.0015	0.40372	1.30181	36.36	5.30212
23.08.2023 19:00	0.01099	0.0015	0.39398	2.46628	21.4	8.90401

Table S5. Continued

23.08.2023 20:00	0.0098	0.00151	0.38424	2.71819	16.52	8.50967
23.08.2023 21:00	0.00936	0.00143	0.37245	2.24242	9.36	8.40142
23.08.2023 22:00	0.00892	0.00135	0.36067	2.77582	9.68	8.24788
24.08.2023 01:00	0.00543	2.70E-04	0.21716	1.53002	6.56	5.4783
24.08.2023 02:00	0.00457	5.30E-04	0.1399	1.25349	10.88	5.61156
24.08.2023 03:00	0.00455	5.40E-04	0.13396	1.48768	12.88	7.10047
24.08.2023 04:00	0.00453	5.60E-04	0.12803	1.47078	12.84	6.31321
24.08.2023 05:00	0.00748	0.00152	0.26221	1.35469	14.04	6.28042
24.08.2023 06:00	0.01042	0.00249	0.39638	1.19363	10.4	8.17877
24.08.2023 07:00	0.01118	0.00351	0.44082	1.75288	7.84	9.31344
24.08.2023 09:00	0.01112	0.0046	0.4362	2.04771	5.68	11.69575
24.08.2023 10:00	0.01029	0.00468	0.38714	1.93393	7.68	9.61557
24.08.2023 11:00	0.0096	0.00407	0.39624	1.84664	7.48	8.41321
24.08.2023 13:00	0.00846	0.00201	0.33299	1.85109	10.68	6.98042
24.08.2023 14:00	0.00801	5.60E-04	0.26064	1.72426	13.8	6.19976
24.08.2023 15:00	0.01036	9.50E-04	0.29205	1.78198	15.24	6.63325
24.08.2023 16:00	0.0127	0.00134	0.32346	1.99735	12.12	9.43113
24.08.2023 19:00	0.01181	0.00226	0.46426	2.90776	5.84	9.57854
25.08.2023 19:00	0.00895	0.00106	0.35015	1.63872	35.8	5.42877

Table S6. Soluble fractions of the transition metals as determined from field measurement studies (Connell et al., 2006; Manousakas et al., 2014; Heal et al., 2005; Giorio et al., 2025).

Soluble fraction	Metal	Reference
0.32	Fe	Giorio et al. (2025)
0.11	Fe	Giorio et al. (2025)
0.21	Fe	Giorio et al. (2025)
0.19	Fe	Giorio et al. (2025)
0.42	Fe	Giorio et al. (2025)
0.28	Fe	Giorio et al. (2025)
0.37	Fe	Giorio et al. (2025)
0.29	Fe	Giorio et al. (2025)
0.15	Fe	Giorio et al. (2025)
0.082	Fe	Giorio et al. (2025)
0.142	Fe	Manousakas et al. (2014)
0.11	Fe	Connell et al. (2006)
0.163	Fe	Heal et al. (2005)
0.2975	Cu	Manousakas et al. (2014)
0.44	Cu	Manousakas et al. (2014)
0.51	Cu	Heal et al. (2005)
0.94	Cu	Connell et al. (2006)
0.1596	Mn	Manousakas et al. (2014)
0.45	Mn	Heal et al. (2005)
Median Fe	0.19	This study
Median Cu	0.48	This study
Median Mn	0.30	This study

3 Supplementary Text

3.1 H_2O_2 production experiments

In order to reproduce the experimental data of Charrier et al. (2014), in addition to the transition metals and quinones, the model includes 300 μM of citric acid, 200 μM ascorbic acid, 100 μM uric acid and 100 μM GSH. The final output is calculated by diving the H_2O_2 concentration at 3600 seconds by 3600, resulting in a production rate of H_2O_2.

3.2 OH production experiments

In order to reproduce the experimental data of Charrier and Anastasio (2015), in addition to the transition metals and quinones, the model includes 300 μM of citric acid, 200 μM ascorbic acid, 100 μM uric acid, 100 μM GSH and 10 mM of Benzoate. The rate of OH production is calculated by taking the linear slope between 0 and 4 hrs.

3.3 Ascorbic acid experiments

In order to reproduce the experimental data of Expósito et al. (2024), in addition to the transition metals and quinones, the model includes an initial concentration of 200 μM ascorbic acid. The simulations are conducted at 310 K.

3.4 DHA production experiments

In order to reproduce the experimental data of Shen et al. (2021), the model include 200 μM of ascorbic acid, and varying concentrations of transition metals. These are allowed to react for 20 mins. The simulations are conducted at 310 K. The oxidation of ascorbic acid is determined by quantifying the oxidation product dehydroascorbic acid (DHA) at the end of the 20 mins.

3.5 DTT experiments with transition metals and quinones

In order to reproduce the experimental data of Charrier and Anastasio (2012) and Xiong et al. (2017), the model includes an initial DTT concentration of 100 μM and varying concentrations of transition metals and quinones. The simulations are conducted at 310 K. To reproduce the data of Expósito et al. (2024), the initial DTT concentration is set to 50 μM, as used in their study. The rate of DTT loss is calculated by taking the linear slope between 0 and 15 mins.

3.6 DTT experiments with SOA

In order to reproduce the experimental data of Tuet et al. (2017), we follow the experimental protocol from Fang et al. (2015). An initial DTT concentration of 0.1 mM is included in the model. The simulations are conducted at 310 K. The rate of DTT loss was determined by taking the linear slope at 0, 4, 13, 23, 30, and 41 mins.

3.7 EPR experiments with SOA

In order to reproduce the experimental data of Tong et al. (2018), we include an initial spin trap concentration of 10 mM, and an SOA concentration between 0 and 4 mM. As the SOA was freshly produced, we assume a low degree of aging, and do the simulations with 10% and 3% peroxide content Wang et al. (2018).

References

Buettner, G. R. and Jurkiewicz, B. A.: Catalytic Metals, Ascorbate and Free Radicals: Combinations to Avoid, Radiation Research, 145, 532–541, https://doi.org/10.2307/3579271, 1996.

Campbell, S. J., Utinger, B., Barth, A., Paulson, S. E., and Kalberer, M.: Iron and Copper Alter the Oxidative Potential of Secondary Organic Aerosol: Insights from Online Measurements and Model Development, Environ. Sci. Technol., 57, 13 546–13 558, https://doi.org/10.1021/acs.est.3c01975, 2023.

Charrier, J. G. and Anastasio, C.: On dithiothreitol (DTT) as a measure of oxidative potential for ambient particles: evidence for the importance of soluble transition metals, Atmos. Chem. Phys., 12, 9321–9333, https://doi.org/10.5194/acp-12-9321-2012, 2012.

Charrier, J. G. and Anastasio, C.: Rates of Hydroxyl Radical Production from Transition Metals and Quinones in a Surrogate Lung Fluid, Environ. Sci. Technol., 49, 9317–9325, https://doi.org/10.1021/acs.est.5b01606, 2015.

Charrier, J. G., McFall, A. S., Richards-Henderson, N. K., and Anastasio, C.: Hydrogen Peroxide Formation in a Surrogate Lung Fluid by Transition Metals and Quinones Present in Particulate Matter, Environ. Sci. Technol., 48, 7010–7017, https://doi.org/10.1021/es501011w, 2014.

Chevallier, E., Jolibois, R., Meunier, N., Carlier, P., and Monod, A.: "Fenton-like" reactions of methylhydroperoxide and ethylhydroperoxide with Fe2+ in liquid aerosols under tropospheric conditions, Atmospheric Environment, 38, 921–933, https://doi.org/10.1016/j.atmosenv.2003.10.027, 2004.

Connell, D. P., Winter, S. E., Conrad, V. B., Kim, M., and Crist, K. C.: The Steubenville Comprehensive Air Monitoring Program (SCAMP): Concentrations and Solubilities of PM2.5 Trace Elements and Their Implications for Source Apportionment and Health Research, J. Air Waste Manag. Assoc., 56, 1750–1766, https://doi.org/10.1080/10473289.2006.10464580, 2006.

Ervens, B., George, C., Williams, J. E., Buxton, G. V., Salmon, G. A., Bydder, M., Wilkinson, F., Dentener, F., Mirabel, P., Wolke, R., and Herrmann, H.: CAPRAM 2.4 (MODAC mechanism): An extended and condensed tropospheric aqueous phase mechanism and its application, Journal of Geophysical Research: Atmospheres, 108, https://doi.org/10.1029/2002JD002202, 2003.

Expósito, A., Maillo, J., Uriarte, I., Santibáñez, M., and Fernández-Olmo, I.: Kinetics of ascorbate and dithiothreitol oxidation by soluble copper, iron, and manganese, and 1,4-naphthoquinone: Influence of the species concentration and the type of fluid, Chemosphere, 361, 142 435, https://doi.org/10.1016/j.chemosphere.2024.142435, 2024.

Fang, T., Verma, V., Guo, H., King, L. E., Edgerton, E. S., and Weber, R. J.: A semi-automated system for quantifying the oxidative potential of ambient particles in aqueous extracts using the dithiothreitol (DTT) assay: results from the Southeastern Center for Air Pollution and Epidemiology (SCAPE), Atmos. Meas. Tech., 8, 471–482, https://doi.org/10.5194/amt-8-471-2015, 2015.

Giorio, C., Borca, C. N., Zherebker, A., D'Aronco, S., Saidikova, M., Sheikh, H. A., Harrison, R. J., Badocco, D., Soldà, L., Pastore, P., Ammann, M., and Huthwelker, T.: Iron Speciation in Urban Atmospheric Aerosols: Comparison between Thermodynamic Modeling and Direct Measurements, ACS Earth Space Chem., 9, 649–661, https://doi.org/10.1021/acsearthspacechem.4c00359, 2025.

Gonzalez, D. H., Diaz, D. A., Baumann, J. P., Ghio, A. J., and Paulson, S. E.: Effects of albumin, transferrin and humic-like substances on iron-mediated OH radical formation in human lung fluids, Free Radical Biology and Medicine, 165, 79–87, https://doi.org/10.1016/j.freeradbiomed.2021.01.021, 2021.

Halliwell, B. and Gutteridge, J. M. C.: Free Radicals in Biology and Medicine, OUP Oxford, Oxford, 2015.

Heal, M. R., Hibbs, L. R., Agius, R. M., and Beverland, I. J.: Total and water-soluble trace metal content of urban background PM10, PM2.5 and black smoke in Edinburgh, UK, Atmos. Environ., 39, 1417–1430, https://doi.org/10.1016/j.atmosenv.2004.11.026, 2005.

Jacobsen, F., Holcman, J., and Sehested, K.: Oxidation of manganese(II) by ozone and reduction of manganese(III) by hydrogen peroxide in acidic solution, International Journal of Chemical Kinetics, 30, 207–214, https://doi.org/10.1002/(SICI)1097-4601(1998)30:3<207::AID-KIN6>3.0.CO;2-W, 1998.

Kemp, T. J.: Kinetic Aspects of Spin Trapping, Progress in Reaction Kinetics, 24, 287–358, https://doi.org/10.3184/007967499103165102, 1999.

Kohen, R. and Nyska, A.: Invited Review: Oxidation of Biological Systems: Oxidative Stress Phenomena, Antioxidants, Redox Reactions, and Methods for Their Quantification, Toxicol Pathol, 30, 620–650, https://doi.org/10.1080/01926230290166724, 2002.

Kumagai, Y., Koide, S., Taguchi, K., Endo, A., Nakai, Y., Yoshikawa, T., and Shimojo, N.: Oxidation of Proximal Protein Sulfhydryls by Phenanthraquinone, a Component of Diesel Exhaust Particles, Chem. Res. Toxicol., 15, 483–489, https://doi.org/10.1021/tx0100993, 2002.

Lakey, P. S. J., Berkemeier, T., Tong, H., Arangio, A. M., Lucas, K., Pöschl, U., and Shiraiwa, M.: Chemical exposure-response relationship between air pollutants and reactive oxygen species in the human respiratory tract, Sci. Rep., 6, 32 916, https://doi.org/10.1038/srep32916, 2016.

Lelieveld, S., Wilson, J., Dovrou, E., Mishra, A., Lakey, P. S. J., Shiraiwa, M., Pöschl, U., and Berkemeier, T.: Hydroxyl Radical Production by Air Pollutants in Epithelial Lining Fluid Governed by Interconversion and Scavenging of Reactive Oxygen Species, Environ. Sci. Technol., 55, 14 069–14 079, https://doi.org/10.1021/acs.est.1c03875, 2021.

Liu, M. J., Wiegel, A. A., Wilson, K. R., and Houle, F. A.: Aerosol Fragmentation Driven by Coupling of Acid–Base and Free-Radical Chemistry in the Heterogeneous Oxidation of Aqueous Citric Acid by OH Radicals, J. Phys. Chem. A, 121, 5856–5870, https://doi.org/10.1021/acs.jpca.7b04892, 2017.

Manousakas, M., Papaefthymiou, H., Eleftheriadis, K., and Katsanou, K.: Determination of water-soluble and insoluble elements in PM2.5 by ICP-MS, Sci. Total Environ., 493, 694–700, https://doi.org/10.1016/j.scitotenv.2014.06.043, 2014.

Morgan, J. J.: Kinetics of reaction between O2 and Mn(II) species in aqueous solutions, Geochimica et Cosmochimica Acta, 69, 35–48, https://doi.org/10.1016/j.gca.2004.06.013, 2005.

Mouchel-Vallon, C., Deguillaume, L., Monod, A., Perroux, H., Rose, C., Ghigo, G., Long, Y., Leriche, M., Aumont, B., Patryl, L., Armand, P., and Chaumerliac, N.: CLEPS 1.0: A new protocol for cloud aqueous phase oxidation of VOC mechanisms, Geosci. Model Dev., 10, 1339–1362, https://doi.org/10.5194/gmd-10-1339-2017, 2017.

Netto, L. E. and Stadtman, E. R.: The Iron-Catalyzed Oxidation of Dithiothreitol Is a Biphasic Process: Hydrogen Peroxide Is Involved in the Initiation of a Free Radical Chain of Reactions, Archives of Biochemistry and Biophysics, 333, 233–242, https://doi.org/10.1006/abbi.1996.0386, 1996.

Pham, A. N., Xing, G., Miller, C. J., and Waite, T. D.: Fenton-like copper redox chemistry revisited: Hydrogen peroxide and superoxide mediation of copper-catalyzed oxidant production, Journal of Catalysis, 301, 54–64, https://doi.org/10.1016/j.jcat.2013.01.025, 2013.

Shen, J., Griffiths, P. T., Campbell, S. J., Utinger, B., Kalberer, M., and Paulson, S. E.: Ascorbate oxidation by iron, copper and reactive oxygen species: review, model development, and derivation of key rate constants, Scientific Reports, 11, 7417, https://doi.org/10.1038/s41598-021-86477-8, 2021.

Sueishi, Y., Hori, M., Ishikawa, M., Matsu-ura, K., Kamogawa, E., Honda, Y., Kita, M., and Ohara, K.: Scavenging rate constants of hydrophilic antioxidants against multiple reactive oxygen species, Journal of Clinical Biochemistry and Nutrition, 54, 67–74, https://doi.org/10.3164/jcbn.13-53, 2014.

Tong, H., Lakey, P. S. J., Arangio, A. M., Socorro, J., Shen, F., Lucas, K., Brune, W. H., Pöschl, U., and Shiraiwa, M.: Reactive Oxygen Species Formed by Secondary Organic Aerosols in Water and Surrogate Lung Fluid, Environ. Sci. Technol., 52, 11 642–11 651, https://doi.org/10.1021/acs.est.8b03695, 2018.

Tuet, W. Y., Chen, Y., Xu, L., Fok, S., Gao, D., Weber, R. J., and Ng, N. L.: Chemical oxidative potential of secondary organic aerosol (SOA) generated from the photooxidation of biogenic and anthropogenic volatile organic compounds, Atmos. Chem. Phys., 17, 839–853, https://doi.org/10.5194/acp-17-839-2017, 2017.

Walling, C.: Some aspects of the chemistry of alkoxy radicals, 15, 69–80, https://doi.org/10.1351/pac196715010069, 1967.

Wang, S., Ye, J., Soong, R., Wu, B., Yu, L., Simpson, A. J., and Chan, A. W. H.: Relationship between chemical composition and oxidative potential of secondary organic aerosol from polycyclic aromatic hydrocarbons, Atmos. Chem. Phys., 18, 3987–4003, https://doi.org/10.5194/acp-18-3987-2018, 2018.

Wei, J., Fang, T., Lakey, P. S. J., and Shiraiwa, M.: Iron-Facilitated Organic Radical Formation from Secondary Organic Aerosols in Surrogate Lung Fluid, Environ. Sci. Technol., 56, 7234–7243, https://doi.org/10.1021/acs.est.1c04334, 2022.

Xiong, Q., Yu, H., Wang, R., Wei, J., and Verma, V.: Rethinking Dithiothreitol-Based Particulate Matter Oxidative Potential: Measuring Dithiothreitol Consumption versus Reactive Oxygen Species Generation, Environ. Sci. Technol., 51, 6507–6514, https://doi.org/10.1021/acs.est.7b01272, 2017.